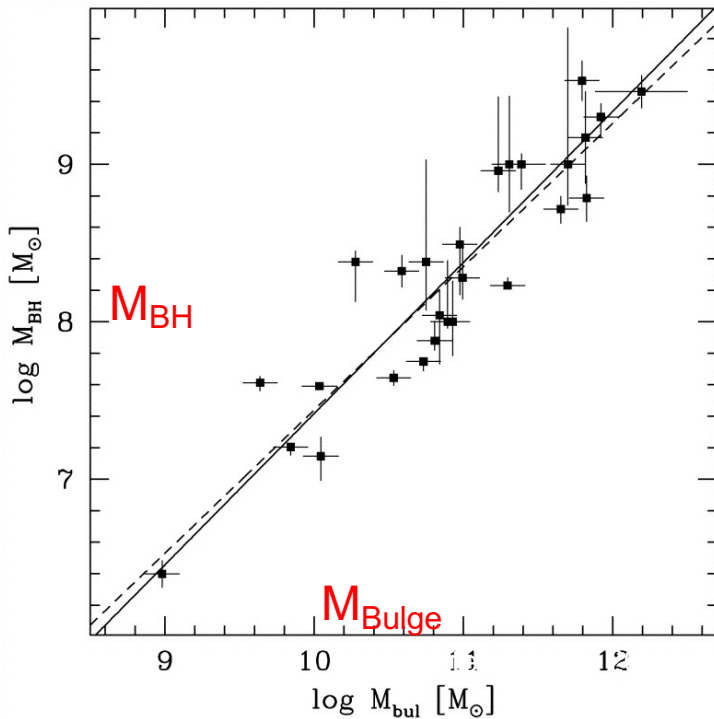


AGN: X-ray surveys and derived evolution

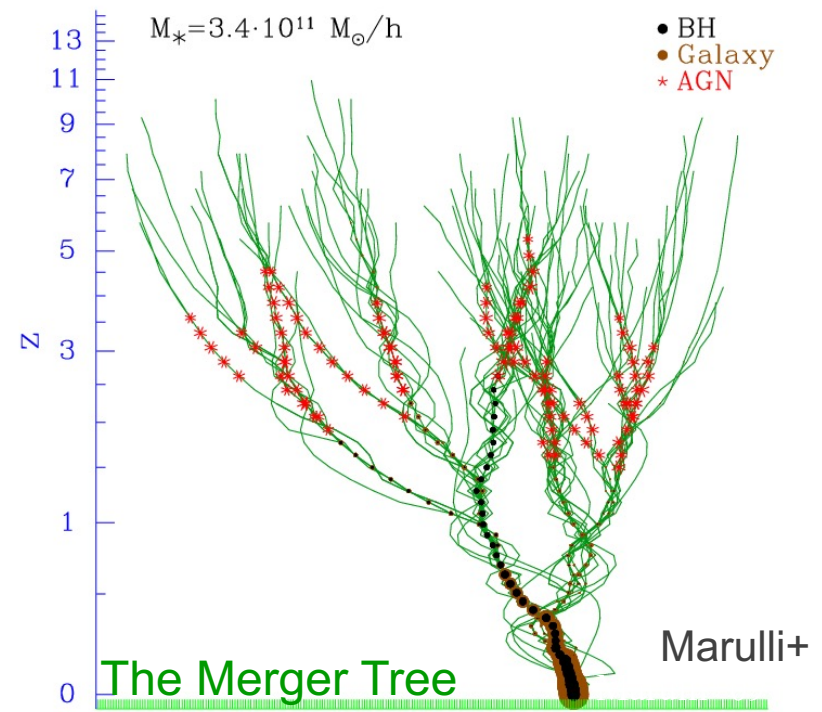
AGN-galaxy co-evolution

BH-galaxy scaling relations. I



Scaling relations between **BH mass**
and **host galaxy properties**
(stellar bulge mass, luminosity,
velocity dispersion)

AGN and galaxies closely tied
→ **co-evolution**



Semi-analytic models of BH/galaxy co-evolution (e.g: Kauffmann+98, Volonteri+06, Salvaterra+06, Rhook&Haehnelt08, Hopkins+08, Menci+08, Marulli+09)

These follow the evolution and merging of Dark Matter Halos with cosmic time and use analytic recipes to treat baryon physics.
Condition: nuclear trigger at merging

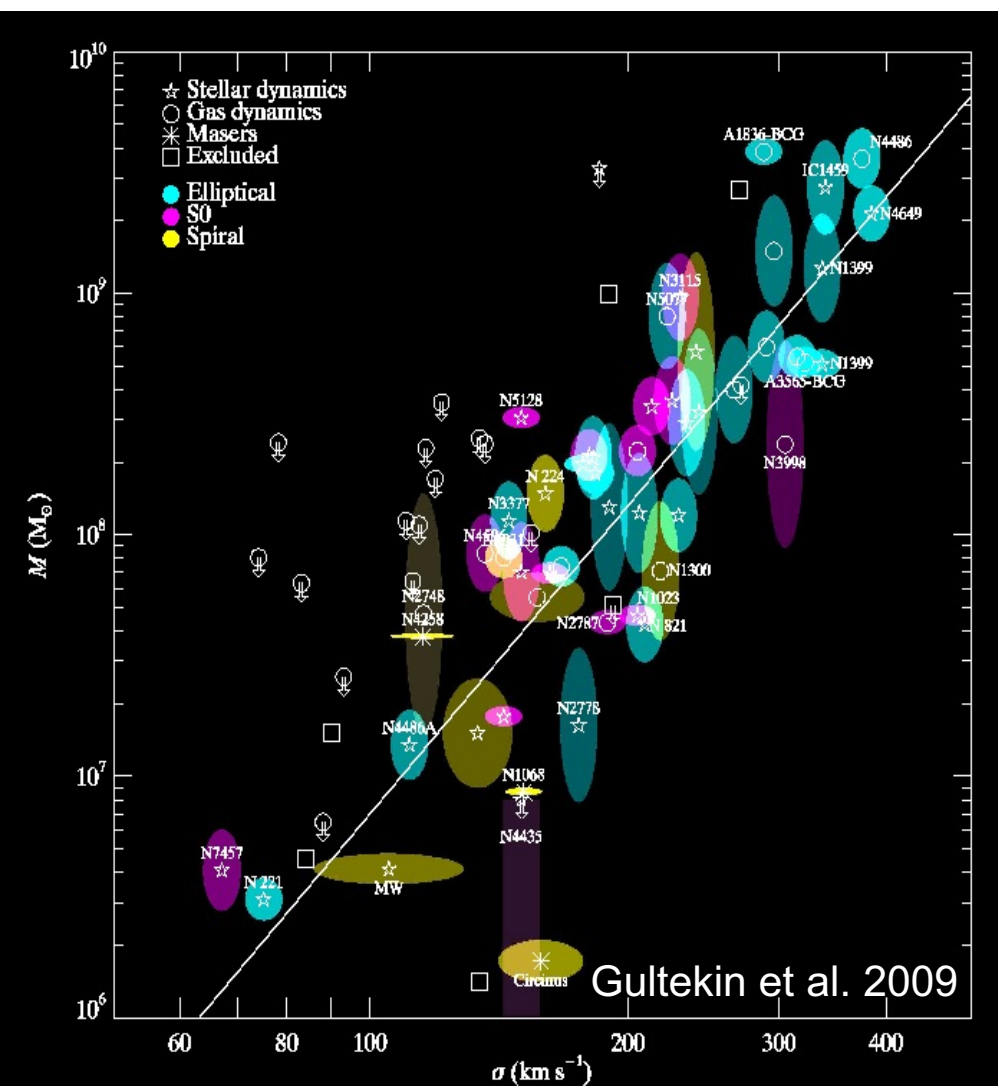
BH-galaxy scaling relations. II

Correlation between BH mass and galaxy velocity dispersion σ

σ measured well **outside** the gravitational sphere of influence of the BH

- No causal connection (now)
- Either coincidence (!) or the result of **common evolution**

Local MBH-galaxy relations are the result of a balance between AGN activity ($L_{\text{Edd}} \sim M_{\text{BH}}$), which tends to expel gas, and galaxy gravitational attraction ($E_{\text{gr}} \sim \sigma^4 R_{\text{e}}$), which tends to retain it. The balance is found for $M_{\text{BH}} \sim 0.001 M_{\text{sph}}$

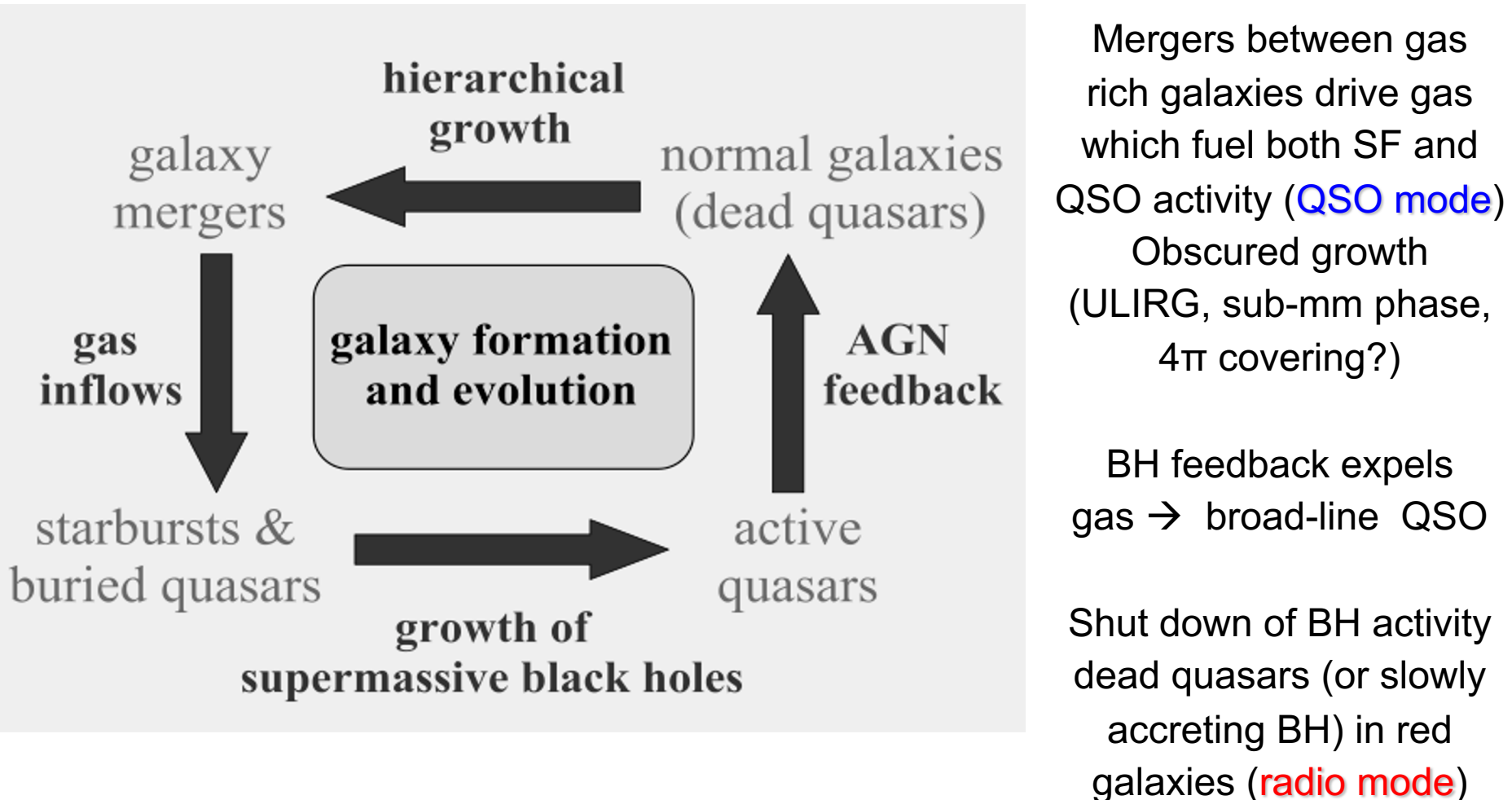


see the review by Kormendy & Ho (2013)

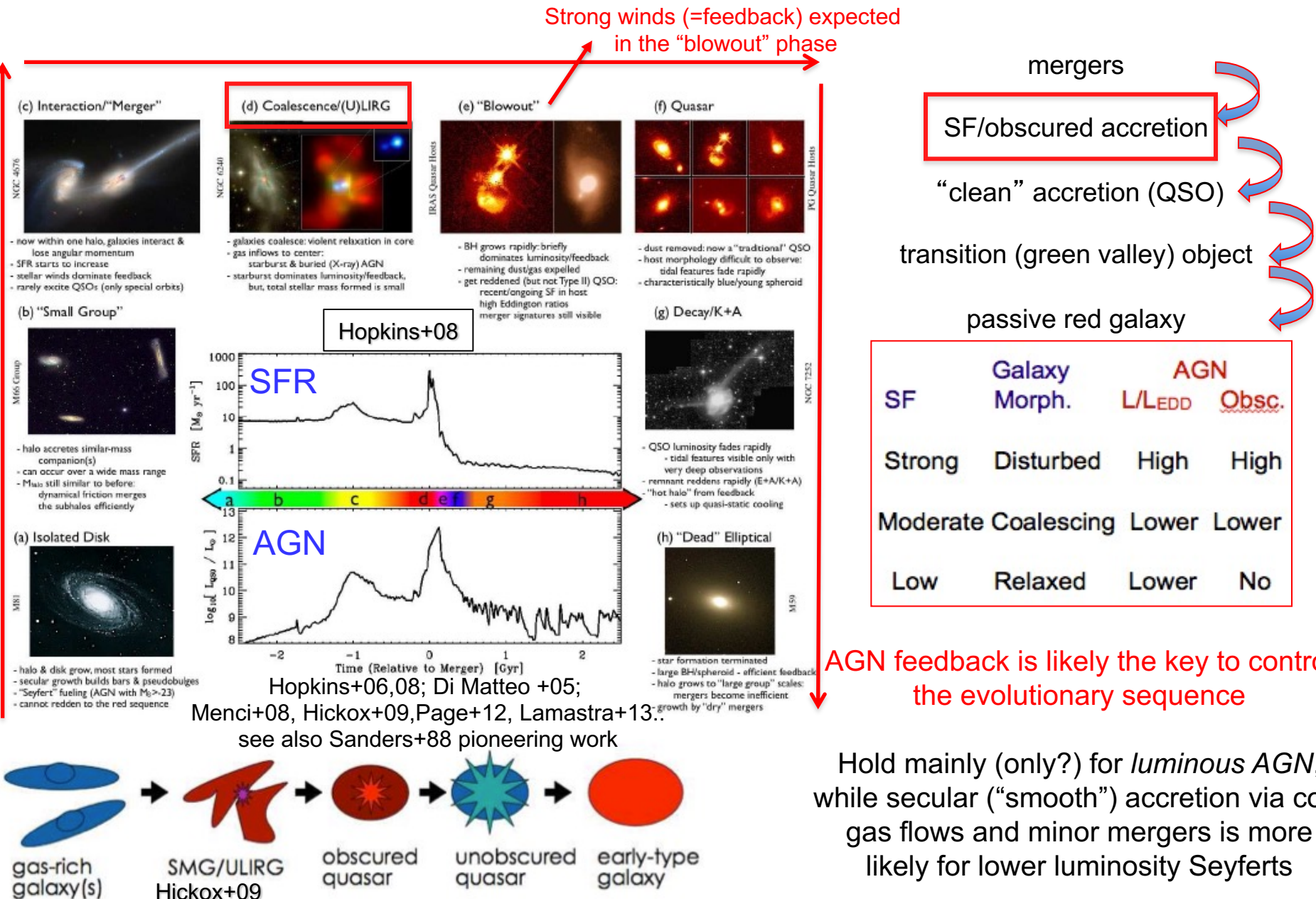
Kormendy and Richstone 1995; Magorrian et al. 1998; Gebhardt et al. 2000; Ferrarese et al. 2000; Tremaine et al. 2002; Gultekin et al. 2009; Kormendy & Bender 2012 – see also Jahnke & Maccio' 2011

The cosmic cycle of galaxy and AGN evolution

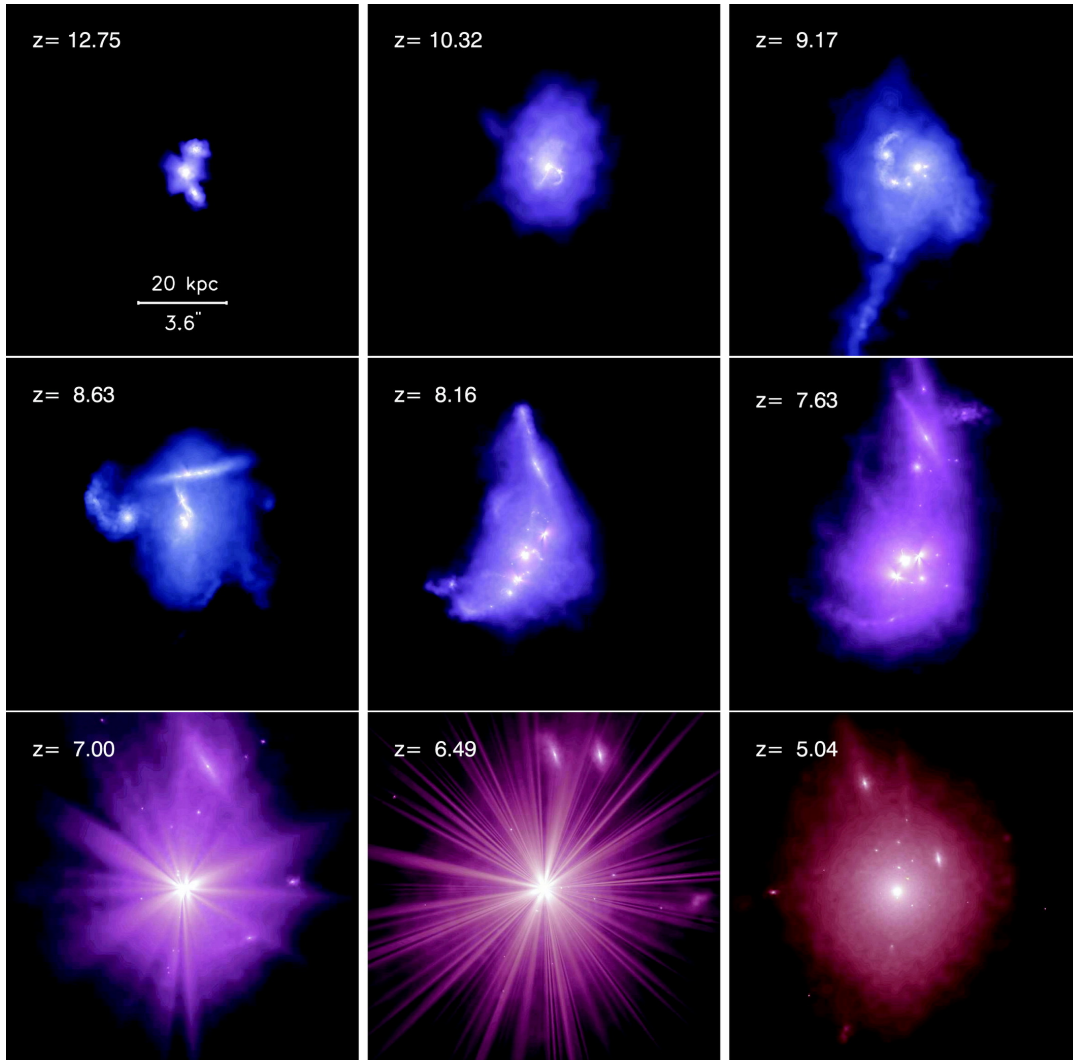
Hopkins et al. 2006



The BH/galaxy evolutionary model



Simulated formation of a $\approx 10^9 M_\odot$ BH at high z

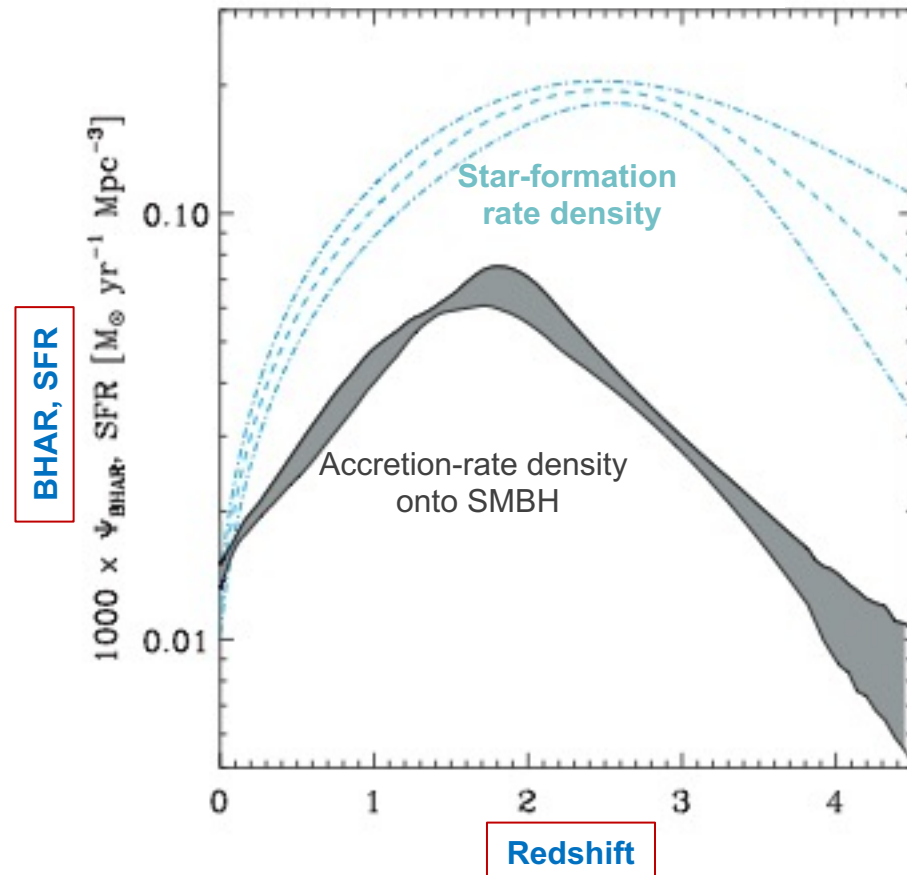


- Early on
 - Strong galaxy interactions= violent star-bursts
 - Heavily obscured QSOs
- When galaxies coalesce
 - accretion peaks
 - QSO becomes optically visible as AGN winds blow out gas
 - outflows as direct evidence for strict QSO/galaxy relation (feedback)
- Later times
 - SF & accretion quenched
 - red spheroid, passive evolution

Li+07

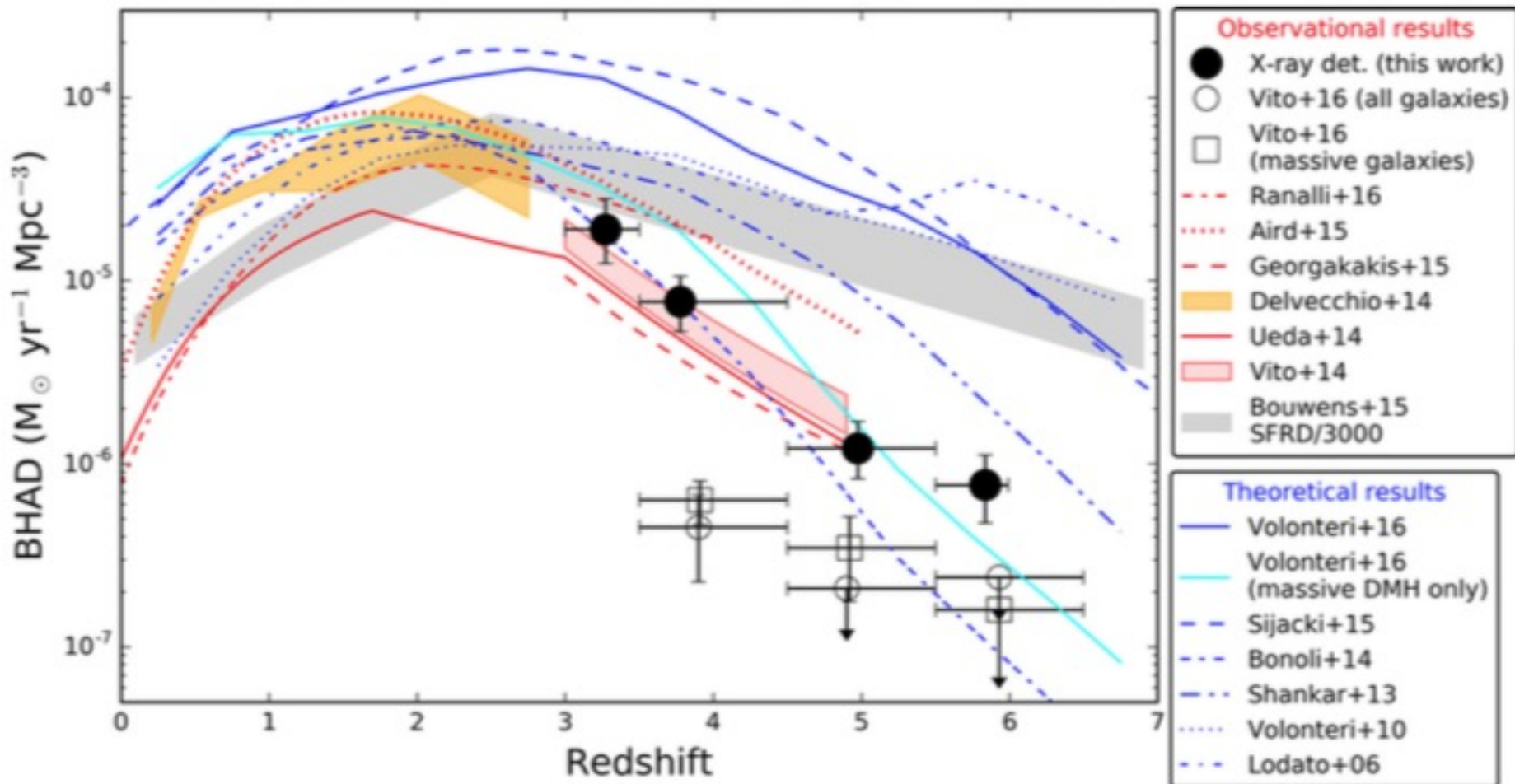
[$M_{\text{BH}} - \sigma$ - M_{Bulge} - ... relations]

Accretion and star formation over cosmic time



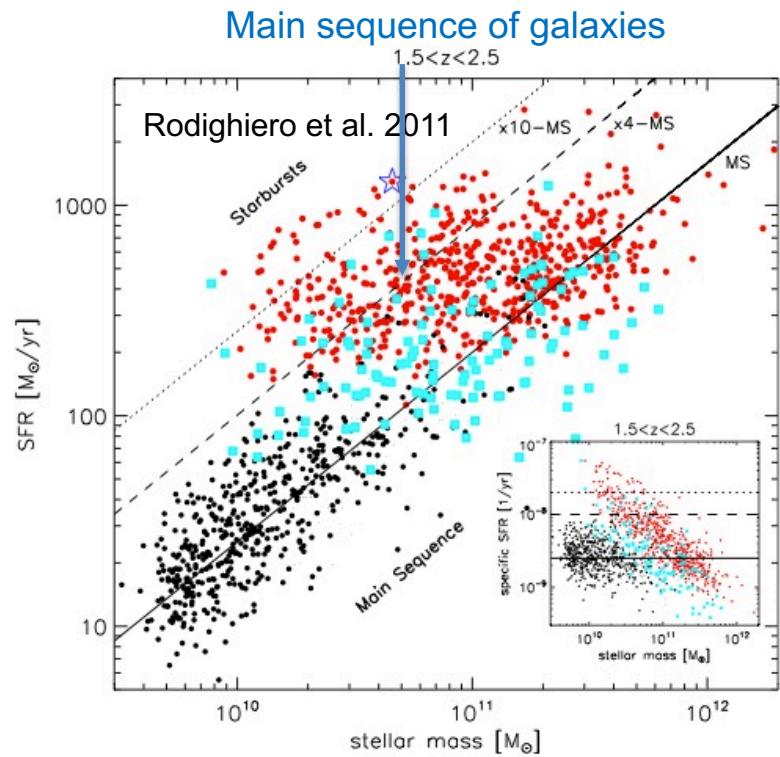
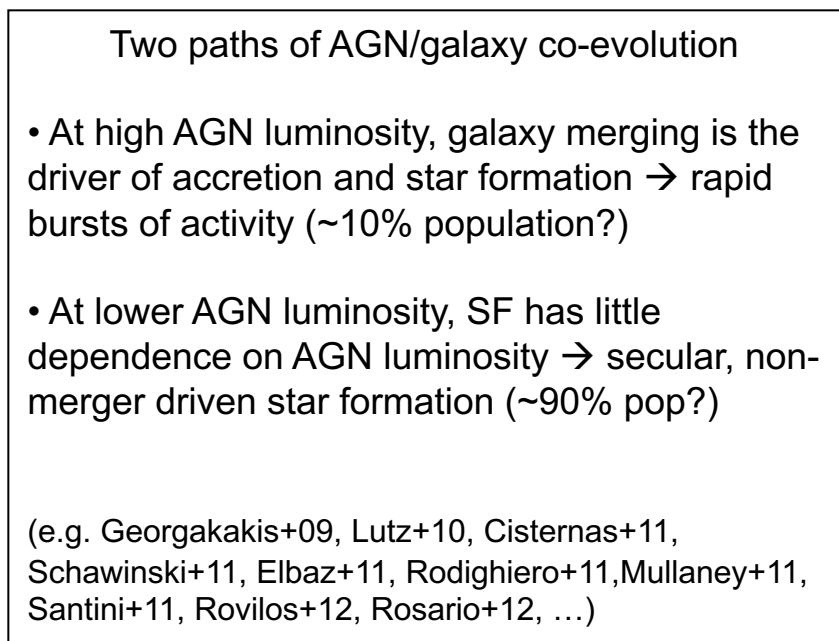
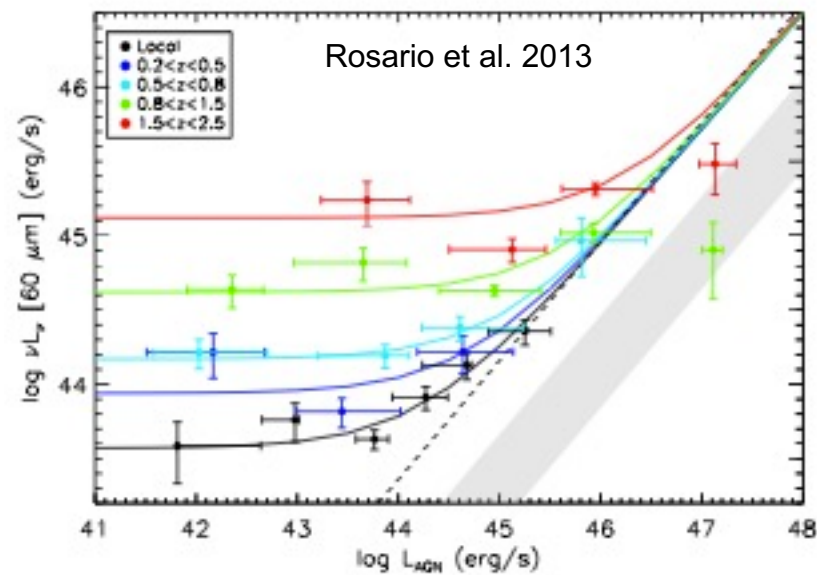
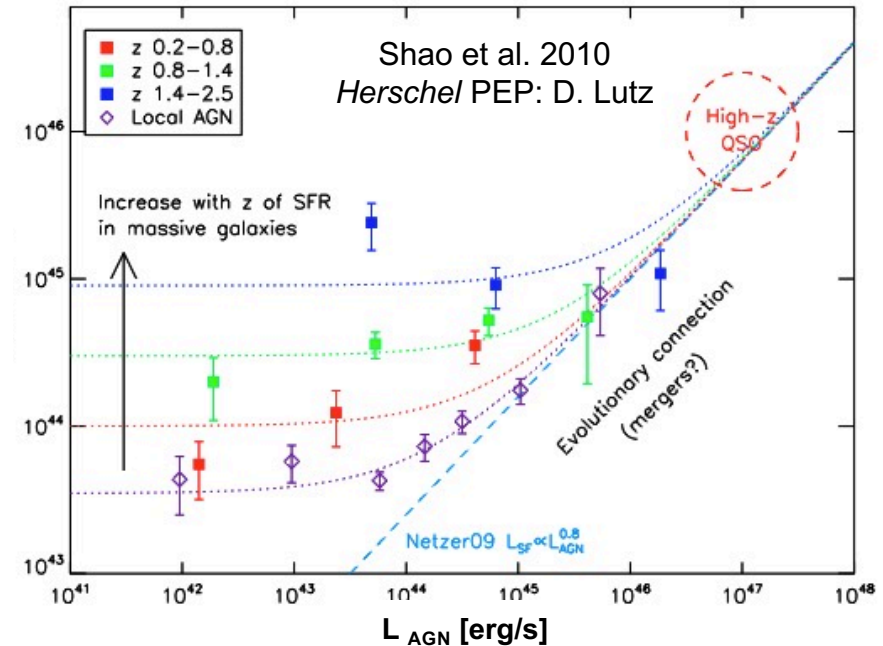
from Merloni & Heinz 2008;
see also Hopkins & Beacom 2006, Gruppioni et al. 2011, Madau et al. 2014

Black hole accretion rate density (BHAD)



Vito et al. (2018)

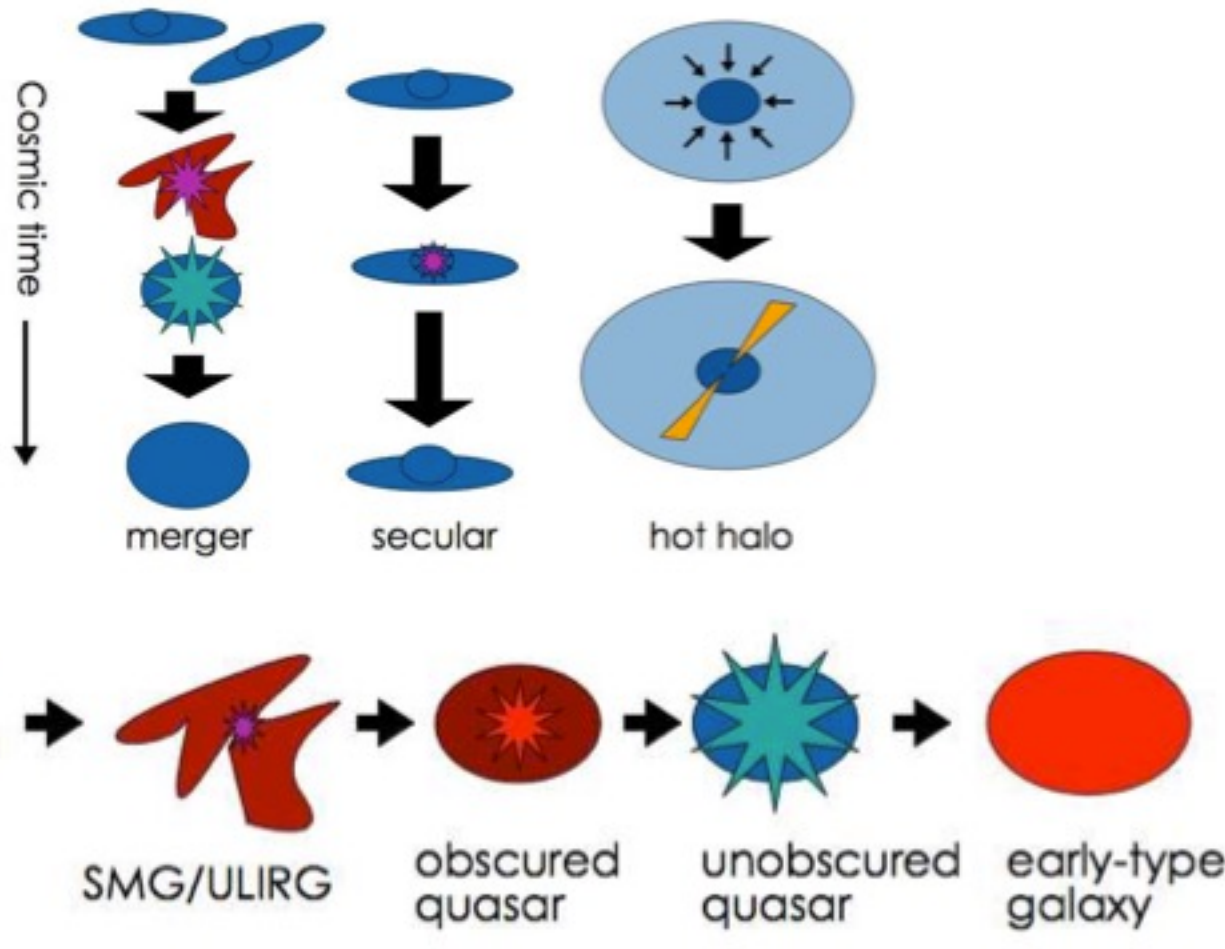
still large uncertainties and observations vs.
model discrepancies



Two modes of accretion

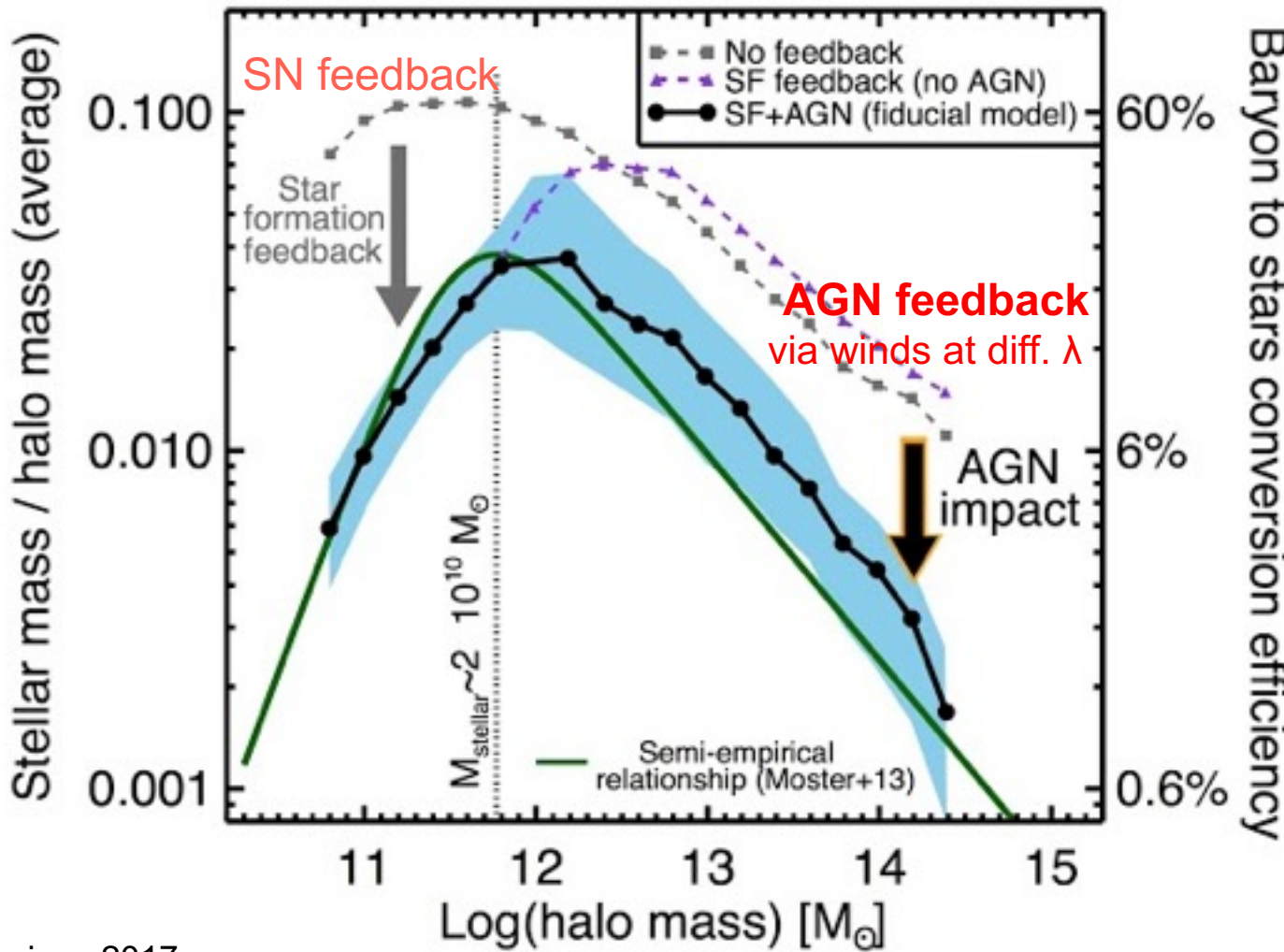
Mergers \longleftrightarrow luminous quasars

Secular (disk instabilities, bars, minor mergers) \longleftrightarrow low-luminosity AGN

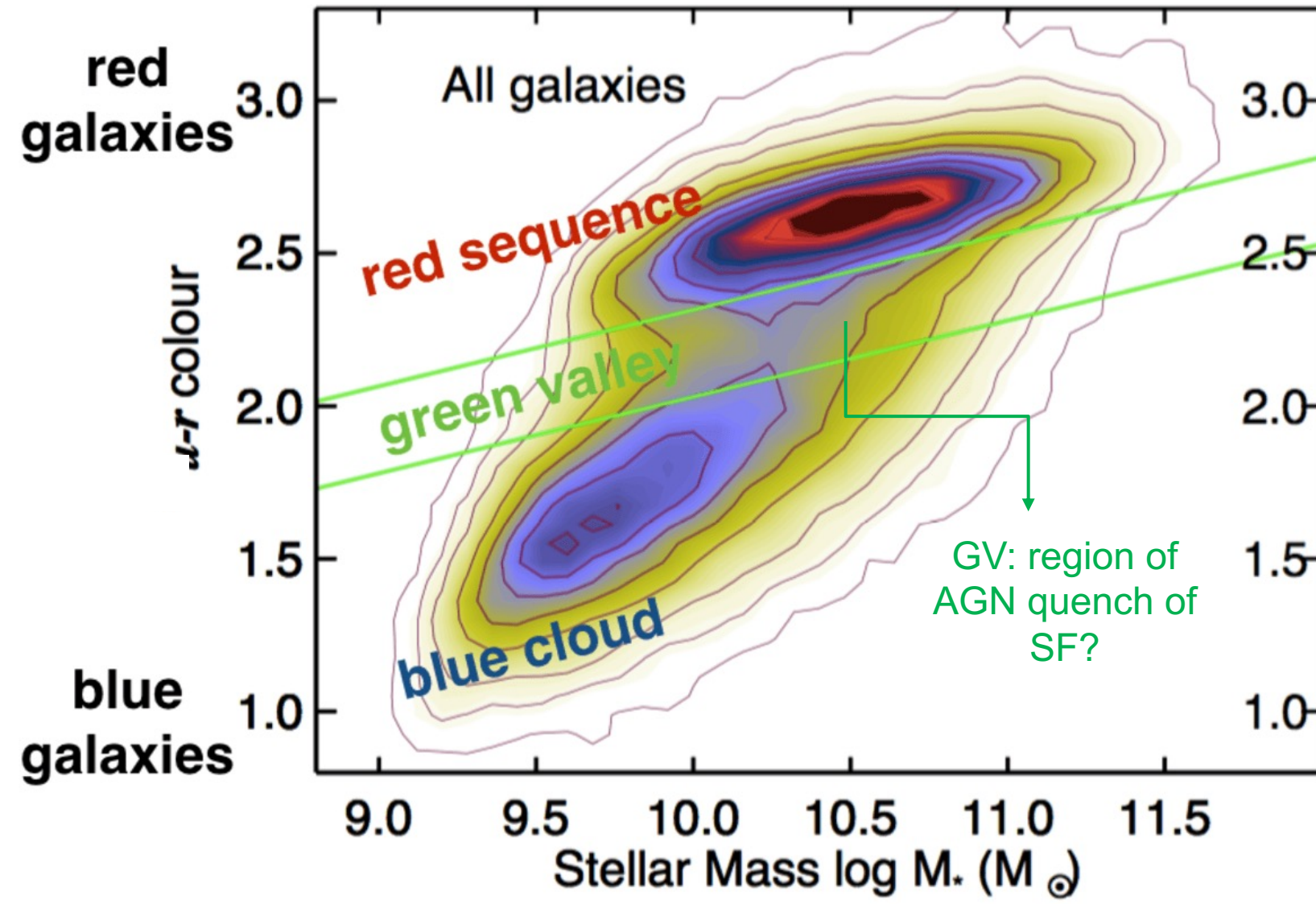


AGN feedback

AGN feedback is needed to explain the galaxy stellar mass function at high masses



Blue vs. red galaxies, and the green valley



Past claims of a higher fraction of AGN activity in the green valley: higher availability of fuel? (Schawinski+10). Then likely quenching of SF \rightarrow galaxy in the red sequence, mostly dry mergers

Obscured AGN growth and star formation at z~2

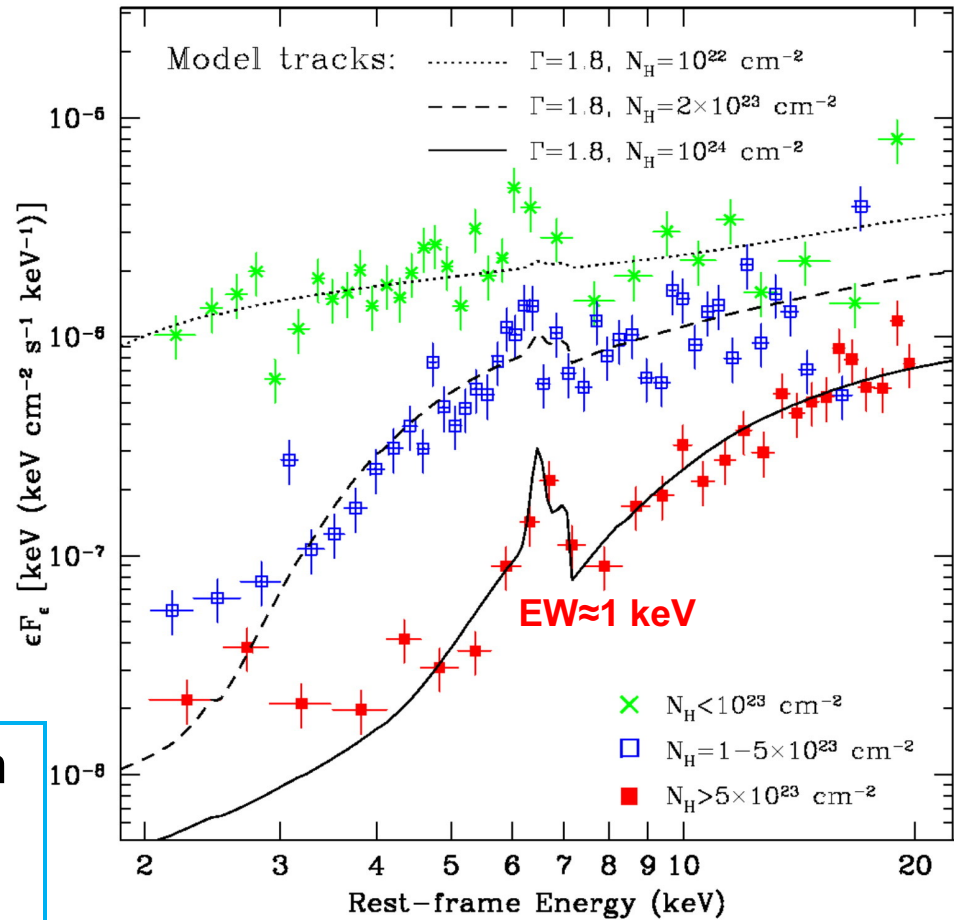
Obscured AGN in sub-mm galaxies

Large reservoir of gas available for accretion and SF

Further indications from mid-IR/optical selected sources

Deep X-ray fields and stacking techniques needed to estimate average source properties

Obscured accretion = key phase in AGN growth and AGN/galaxy co-evolution → Much of the mass growth of SMBH occurs during the heavily obscured phase (e.g., Treister+10)



Alexander et al. 2005

→ Needed: census and knowledge of Compton-thick AGN

Storing the accretion history of the Universe in the X-ray background (XRB), and the role of X-ray surveys

Two hot topics in AGN demography studies

High-redshift

(discussed later in the course)

BH/galaxy co-evolution
still unconstrained at very
high-z ($z>6$ or so).

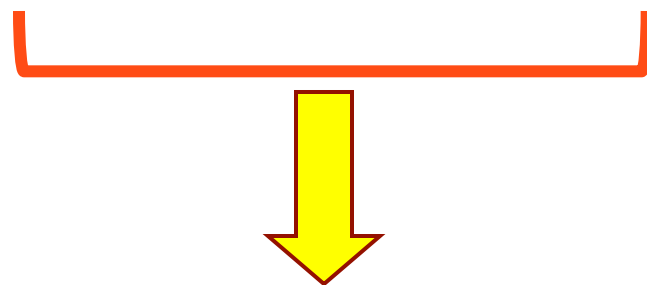
Already formed luminous
QSOs at $z=6-7$

Heavily obscured

AGN

(already discussed, high-z
implications later in the course)

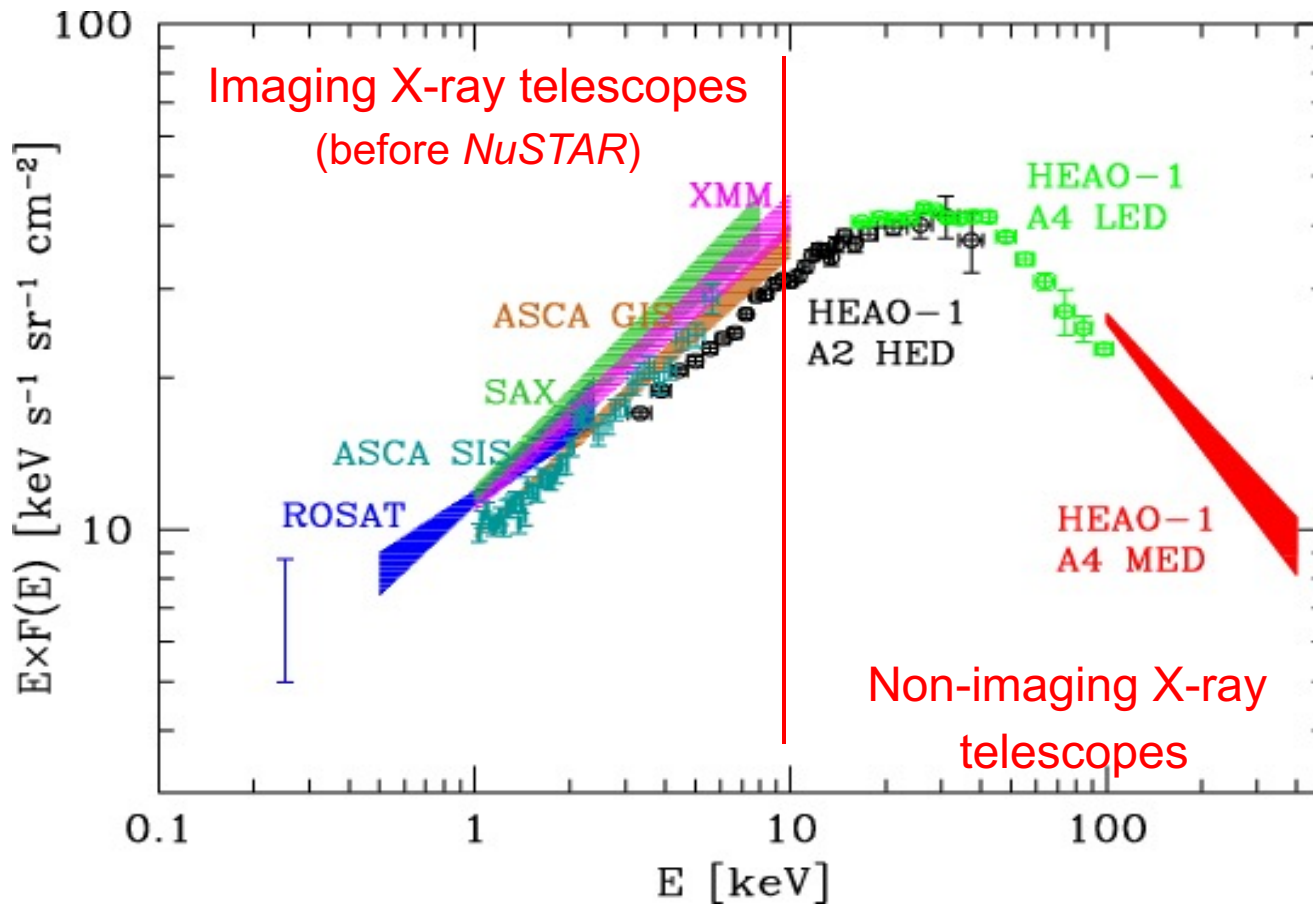
Heavily obscured accretion
mostly unconstrained
beyond the local Universe



Requirement: a complete census of AGN activity

Information stored in the X-ray background

The spectrum of the cosmic XRB



The first spectral data (1980) in the 3-60 keV band could be reproduced accurately by thermal emission from an optically thin plasma:

$$F(E) \approx E^{-0.29} e^{-E/41\text{keV}} \text{ (bremsstrahlung)}$$

Can a diffuse plasma emission explain the XRB?

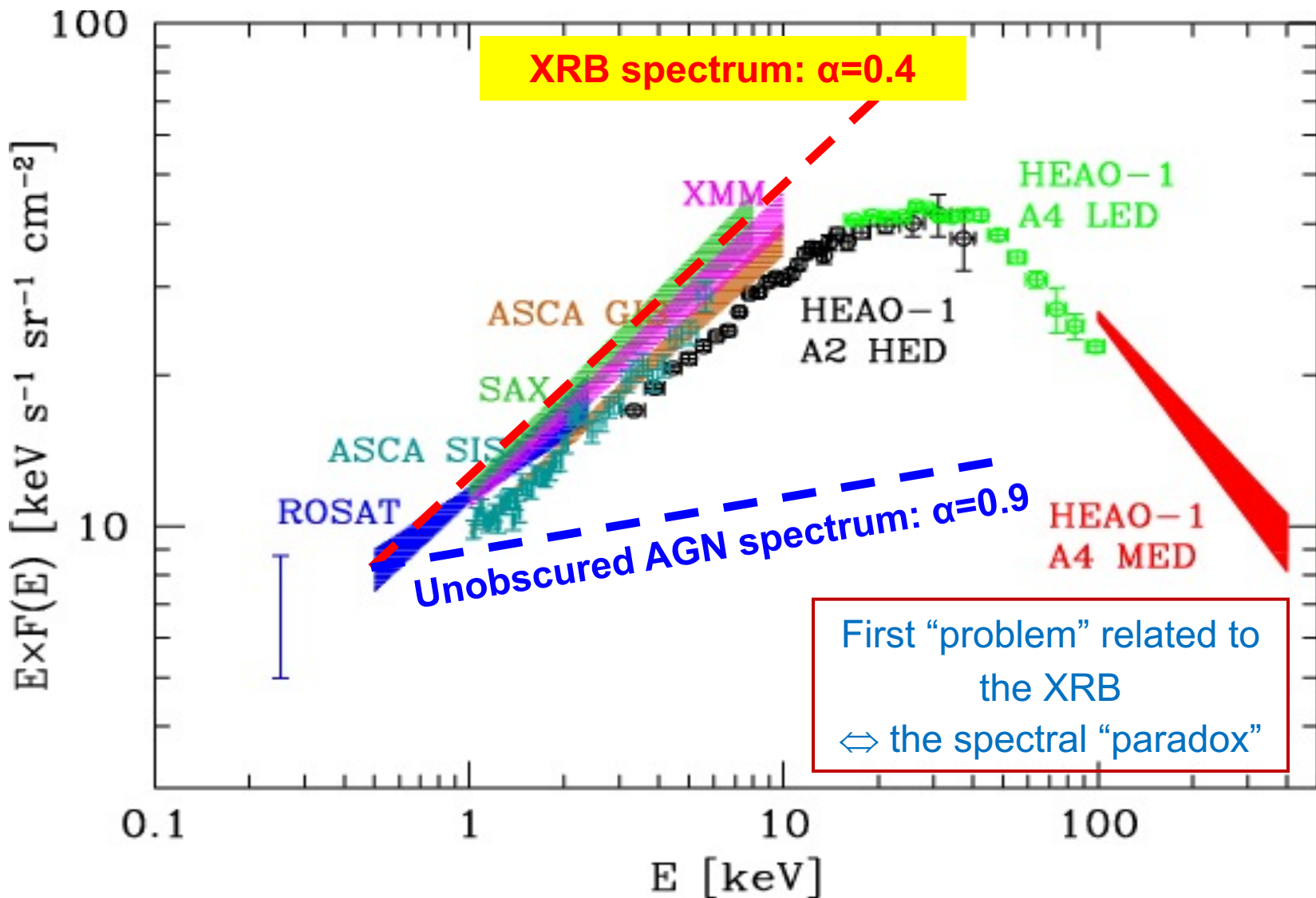
No!

- Subtracting AGN implies an XRB spectrum no more compatible with bremsstrahlung emission
- CMB represents a perfect blackbody; hot gas ($T \sim 40 \text{ keV} \approx 4 \times 10^8 \text{ K}$) would produce distortions by inverse Compton effect (Mather et al. 1994)



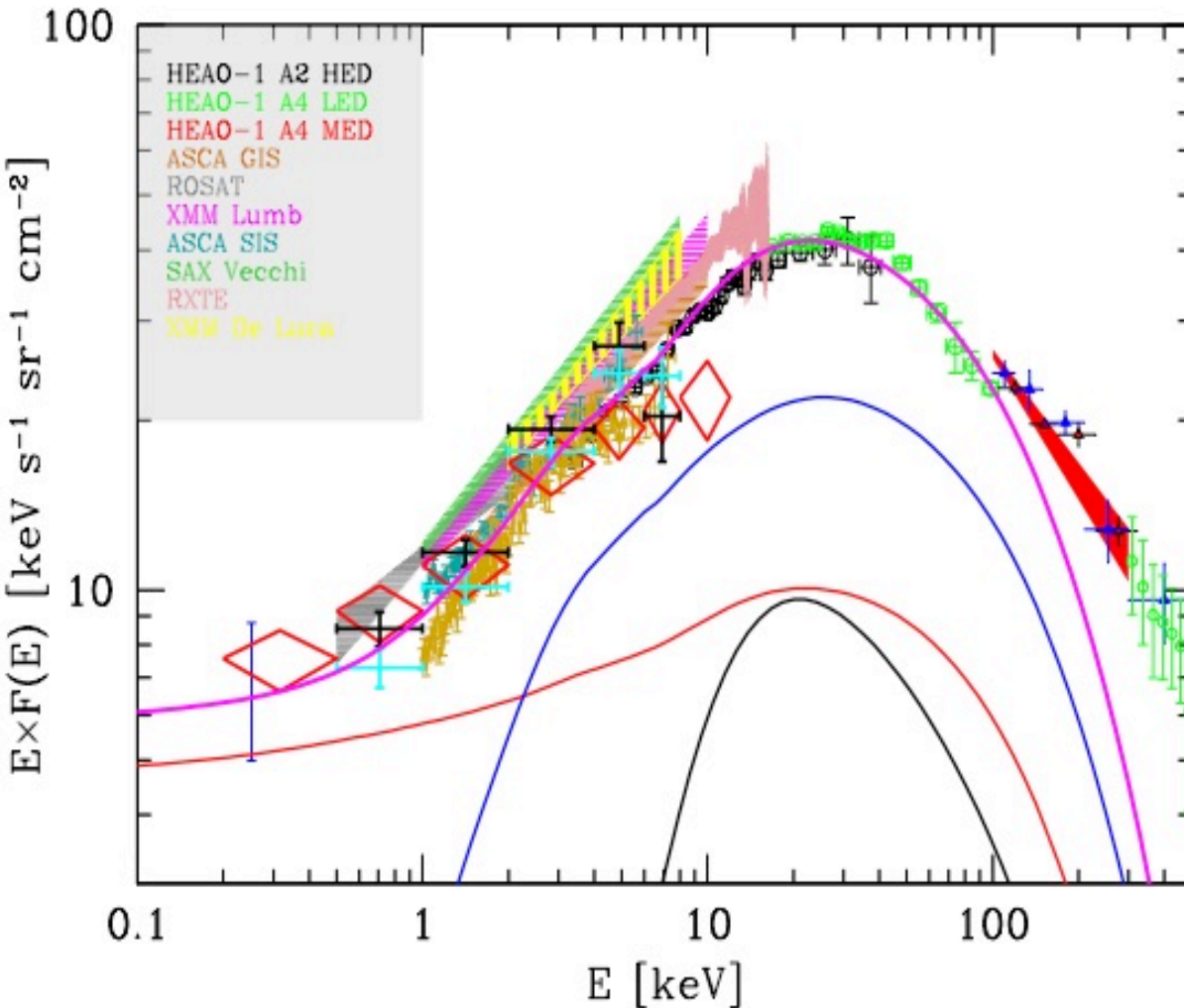
Emission by unresolved, faint individual sources → AGN

The spectral “paradox”



The spectrum of the cosmic XRB

XRB as the ‘sum’ of obscured and unobscured AGN – currently, many models for the XRB, following the original idea of Setti & Woltjer 1989



The **XRB** synthesis provides an integral constraint
(Gilli et al. 2007)

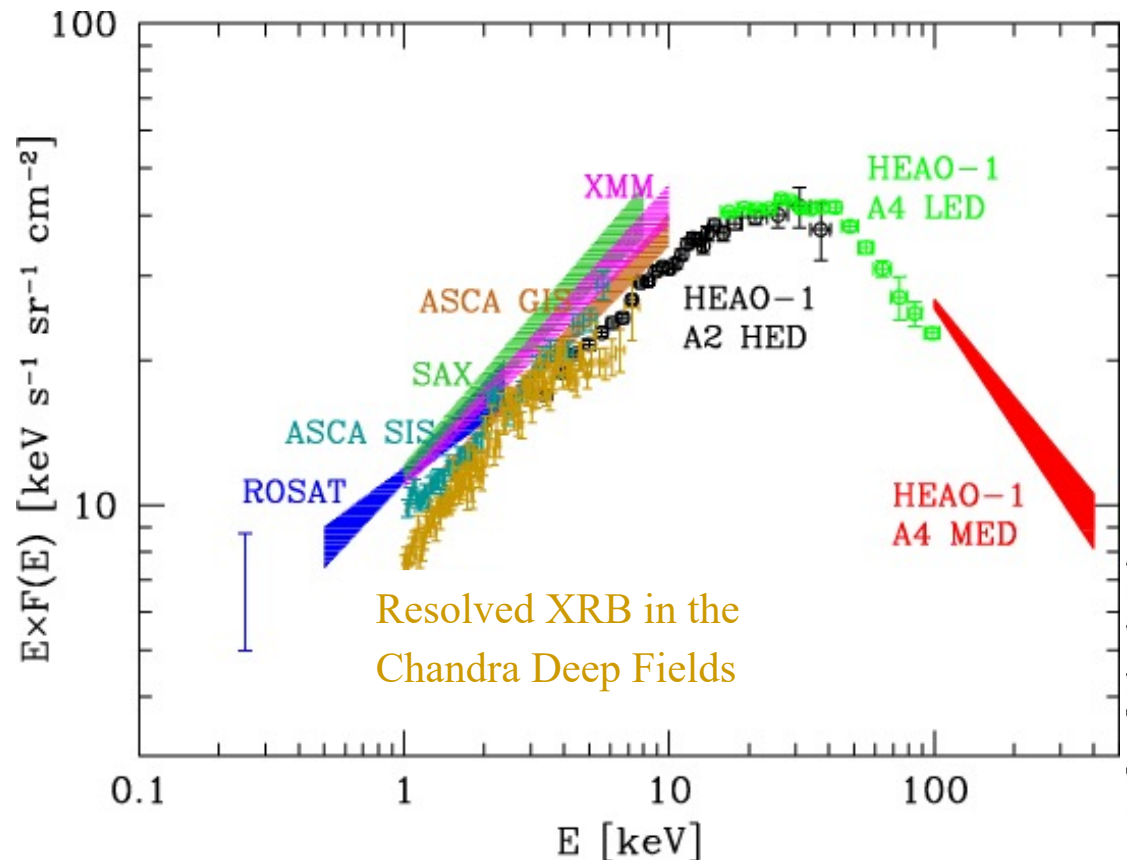
Red → unobscured

Blue → Compton Thin

Black → Compton Thick
($N_H > 10^{24}$ cm⁻²)

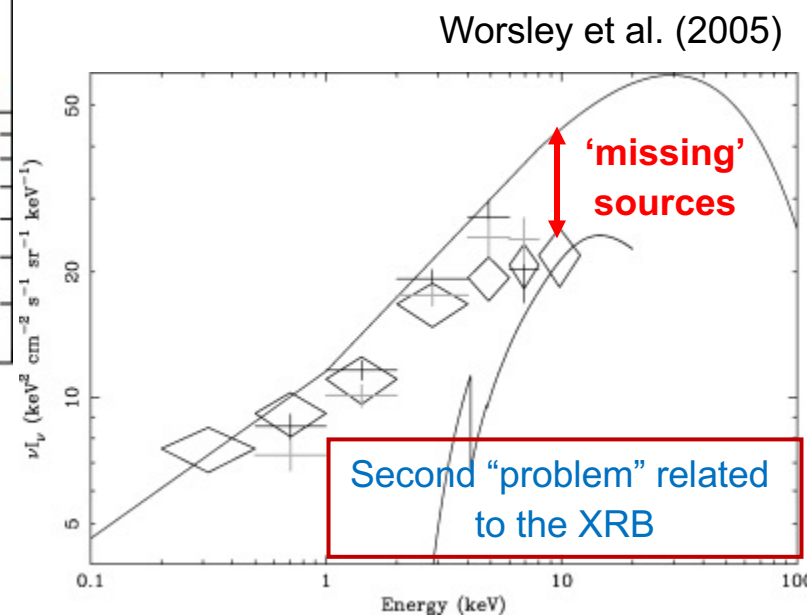
The evolution is folded in the adopted XLF

Resolved XRB fraction: still a “missing” population?



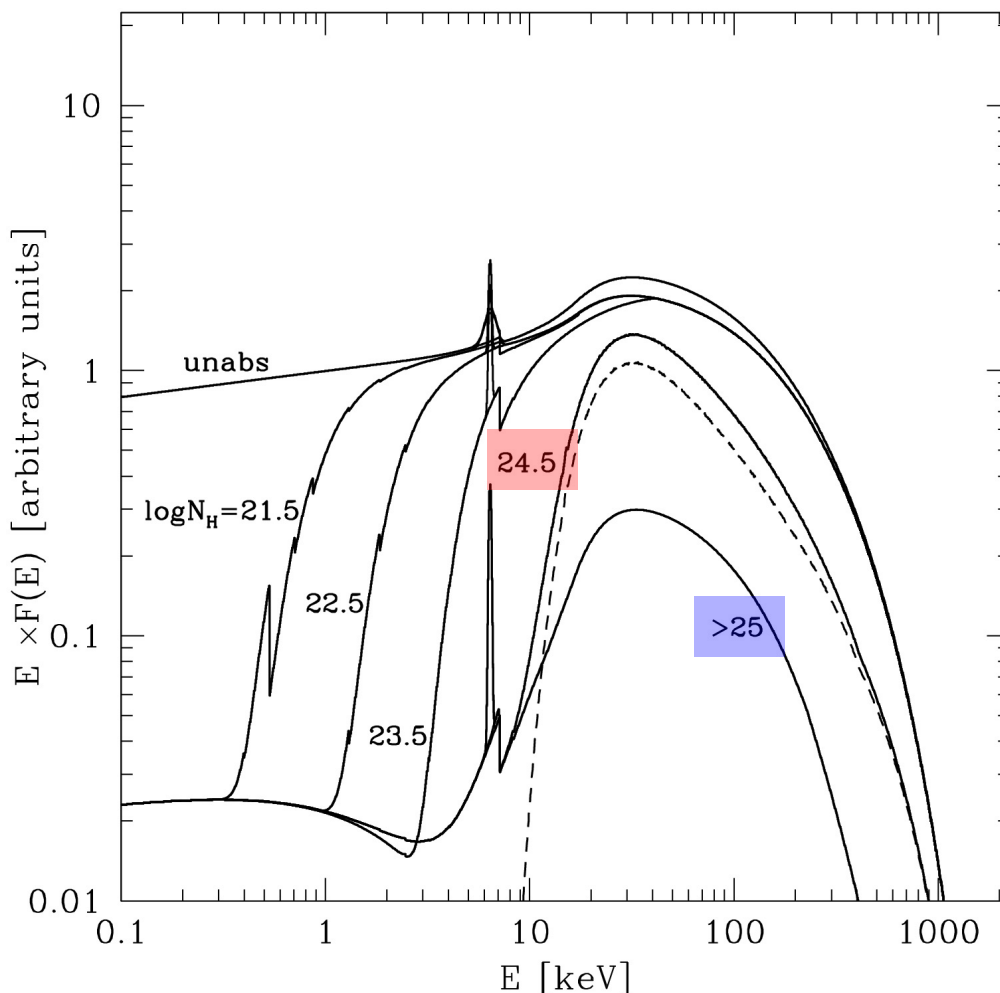
≈50-80% of the XRB being resolved into single sources at $E < 10$ keV
(up to ≈95% in the CDF-S)

BUT only ≈50% resolved above 5 keV



The situation in the last 20 years has largely improved in finding very obscured sources (see the “Obscured AGN” lesson), still significant multi-wavelength efforts need to be done

AGN X-ray spectral templates with different N_{H}



Likely around one hundred “secure” (i.e., with broad-band X-ray data available) Compton-thick AGN known at present. Most of them are local AGN

Unabsorbed:

$$\log N_{\text{H}} < 21$$

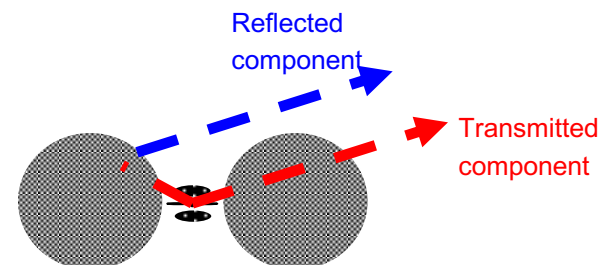
Compton-Thin

$$21 < \log N_{\text{H}} < 24$$

Compton-Thick:

Mildly ($\log N_{\text{H}} = 24-25$)

Heavily ($\log N_{\text{H}} > 25$)

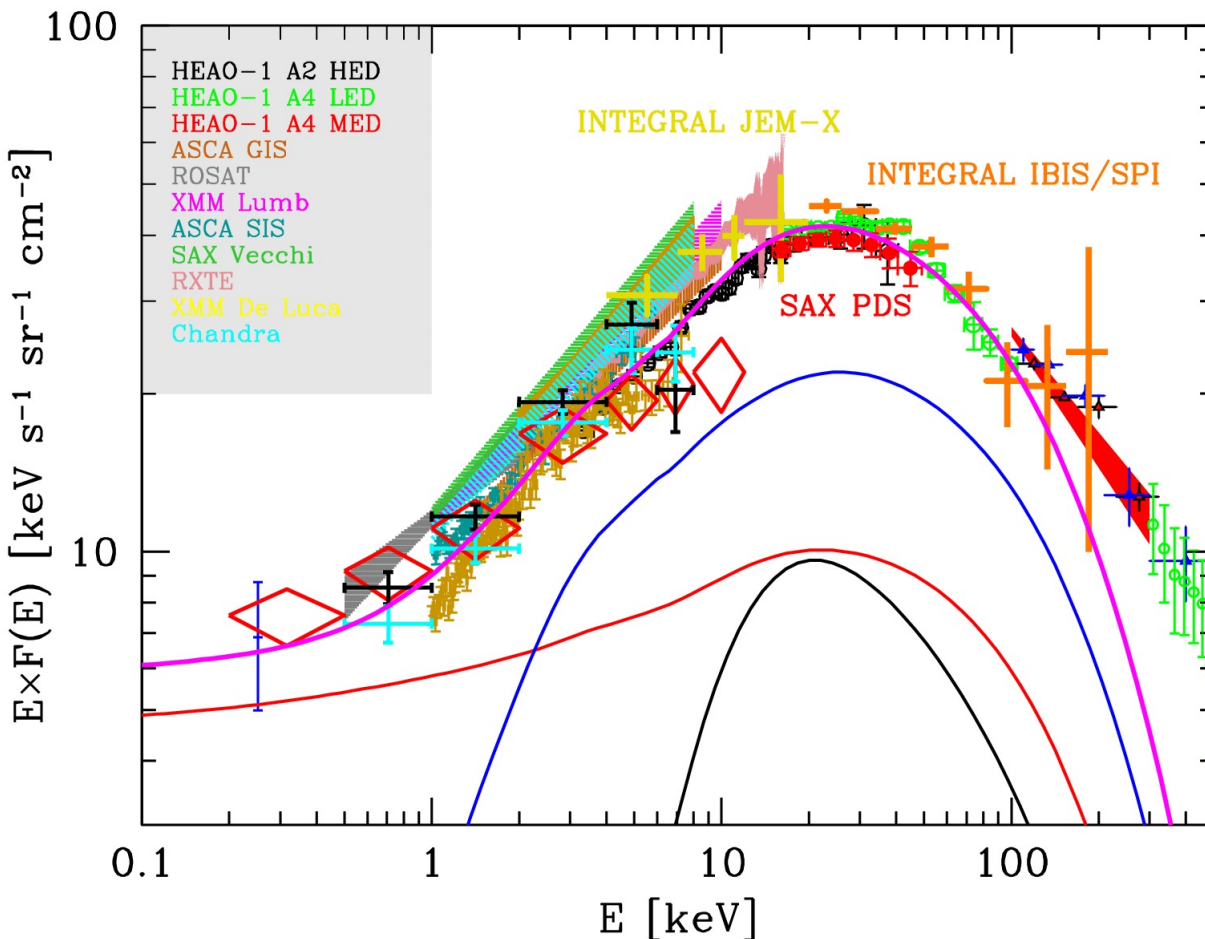


The cold gas in the torus contributes to the iron $\text{K}\alpha$ line emission.

As N_{H} increases, the spectrum is absorbed towards higher and higher energies.

Fitting the XRB with AGN synthesis model

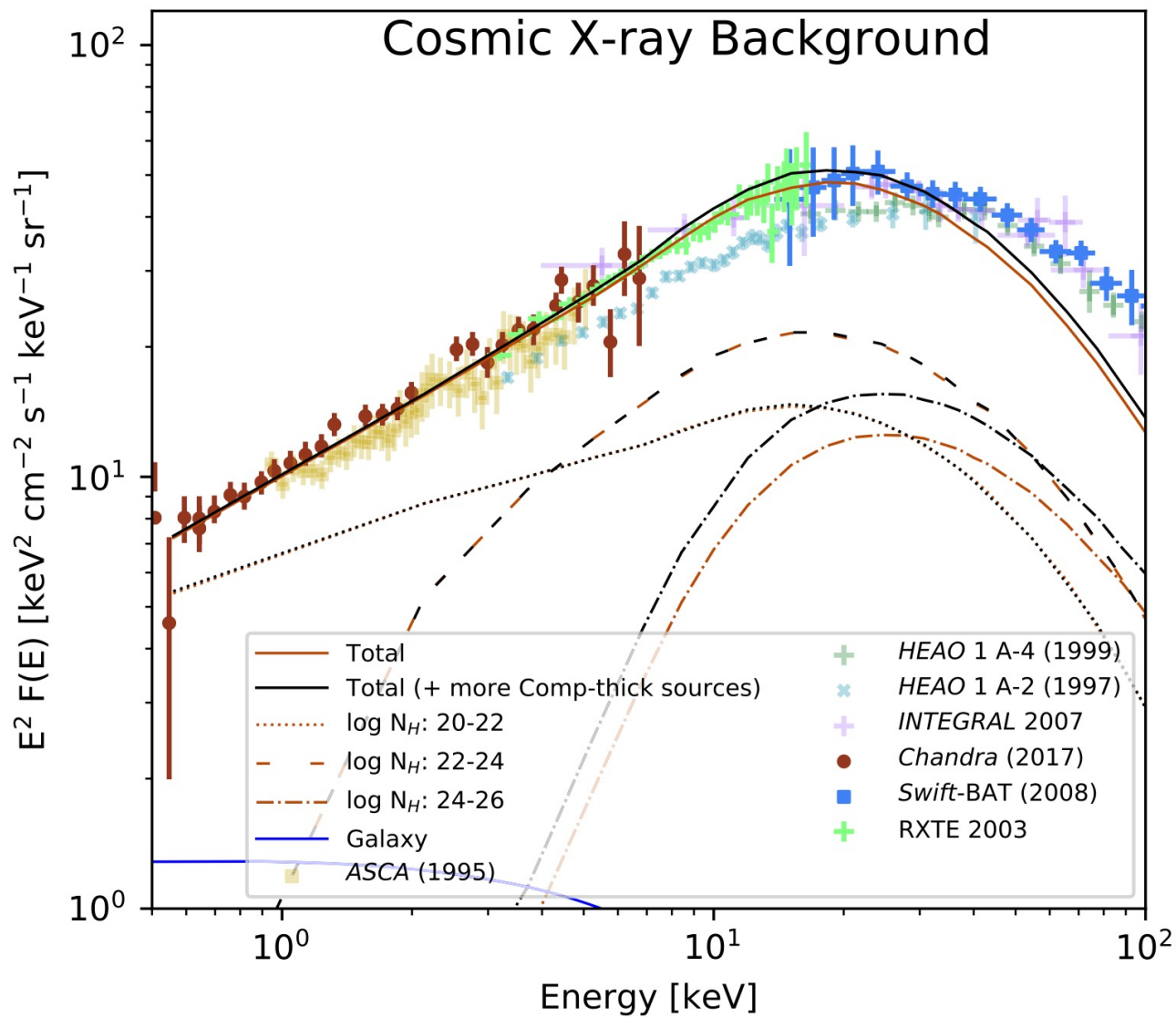
(Gilli et al. 2007)



Now: imaging by *NuSTAR* above 10 keV (limited sens., still limited fraction of resolved XRB)

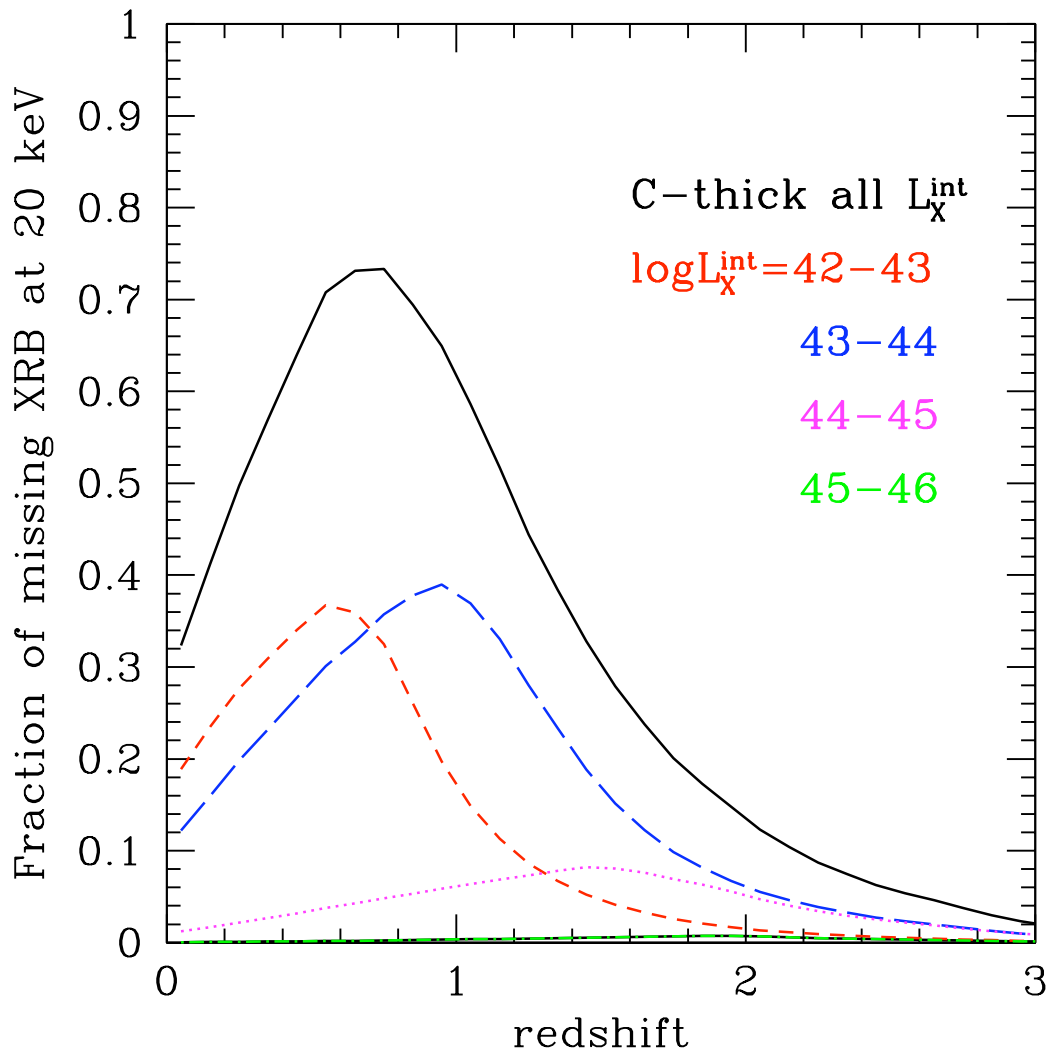
In Gilli+07 model:

- Number of Compton-thin AGN=number of Compton-thick AGN at high L_X
- Compton-thick AGN fill the 30 keV “gap”



Ananna et al. (2020)

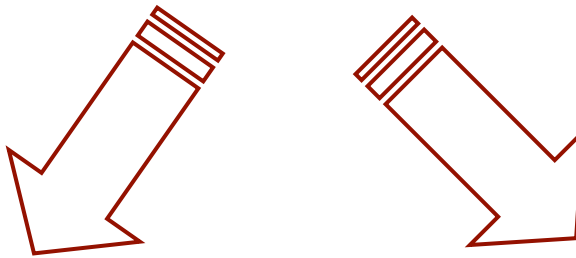
When the “missing” XRB was emitted?



Predicted peak
at $z \approx 0.7 - 0.8$,
mostly at
 $L_x \sim 10^{42-44}$ erg/s

Gilli 2013

Way to provide a census of AGN activity: X-ray surveys



Large-area surveys

to pick up luminous and rare AGN

Relatively bright optical counterparts,
easier optical IDs

Deep-area survey

to pick up faint and distant AGN

Typically faint optical
counterparts, difficult optical IDs

What is the best observing strategy for X-ray surveys?

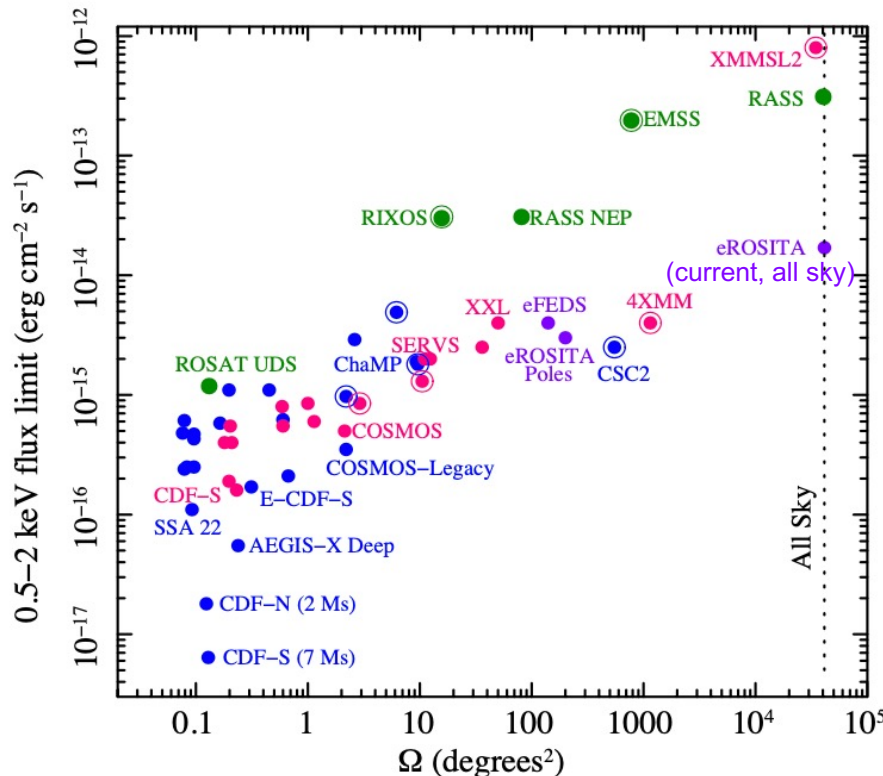
DEEP X-RAY SURVEYS

PROs:

- Ideal to reveal distant sources (because of the depth of the exposure)
- Large number of sources

CONs

- Limited to small areas
- Limited individual photon statistics



Brandt & Yang 2021 (review)

LARGE (and SHALLOW) X-RAY SURVEYS

PROs:

- Ideal to pick up bright and rare X-ray sources
- Possibility to cover large areas of the sky

CONs

- Limited number of sources

Goal: going deep on large area (BUT huge amounts of exposure time would be needed, so not practicable at present)

Table 1 Selected extragalactic X-ray surveys with *Chandra*, *XMM-Newton*, and *NuSTAR*

Survey name	Rep. Eff. Exp. (ks)	Solid angle (arcmin 2)	Representative reference
<i>Chandra</i> (0.3–8 keV)			
	Exposure	Area	
<i>Chandra</i> Deep Field-South (CDF-S)	3870	465	Xue et al. (2011)
<i>Chandra</i> Deep Field-North (CDF-N)	1950	448	Alexander et al. (2003)
AEGIS-X Deep	800	860	Goulding et al. (2012)
SSA22 protocluster	392	330	Lehmer et al. (2009a)
HRC Lockman Hole	300	900	PI: S.S. Murray
Extended CDF-S (E-CDF-S)	250	1,128	Lehmer et al. (2005)
AEGIS-X	200	2,412	Laird et al. (2009)
Lynx	185	286	Stern et al. (2002)
LALA Cetus	174	297	Wang et al. (2007)
LALA Boötes	172	346	Wang et al. (2004)
C-COSMOS and COSMOS-Legacy	160	6,120	Elvis et al. (2009)
SSA13	101	345	Barger et al. (2001b)
Abell 370	94	345	Barger et al. (2001a)
3C 295	92	274	D'Elia et al. (2004)
ELAIS N1+N2	75	590	Manners et al. (2003)
WHDF	72	286	Bielby et al. (2012)
CLANS (Lockman Hole)	70	2,160	Trouille et al. (2008)
SEXEI ^a	45	7,920	Harrison et al. (2003)
CLASXS (Lockman Hole)	40	1,620	Trouille et al. (2008)
13 h Field	40	710	McHardy et al. (2003)
ChaMP ^a	25	34,560	Kim et al. (2007)
XDEEP2 Shallow	15	9,432	Goulding et al. (2012)
<i>Chandra</i> Source Catalog (CSC) ^a	13	1,150,000	Evans et al. (2010)
Stripe 82X– <i>Chandra</i> ^a	9	22,320	LaMassa et al. (2013b)
NDWFS XBoötes	5	33,480	Murray et al. (2005)
<i>XMM-Newton</i> (0.2–12 keV)			
<i>Chandra</i> Deep Field-South (CDF-S)	2820	830	Ranalli et al. (2013)
Lockman Hole	640	710	Brunner et al. (2008)
<i>Chandra</i> Deep Field-North (CDF-N)	180	752	Miyaji et al. (2003)
13 h Field	120	650	Loaring et al. (2005)
ELAIS-S1	90	2,160	Puccetti et al. (2006)
Groth-Westphal	81	730	Miyaji et al. (2004)
COSMOS	68	7,670	Cappelluti et al. (2009)
Subaru <i>XMM-Newton</i> Deep Survey (SXDS)	40	4,100	Ueda et al. (2008)
Marano field	30	2,120	Lamer et al. (2003)
HELLAS2XMM ^a	25	10,440	Baldi et al. (2002)
XMM-LSS XMDS	23	3,600	Chiappetti et al. (2005)

efforts of the last ~20 years
with major X-ray facilities

(Brandt & Alexander 2015)

Going large and deep is the dream
Most of the time: either shallow on
deg 2 regions or deep in sub-deg 2
areas

Similarly in the future with next-
generation X-ray facilities

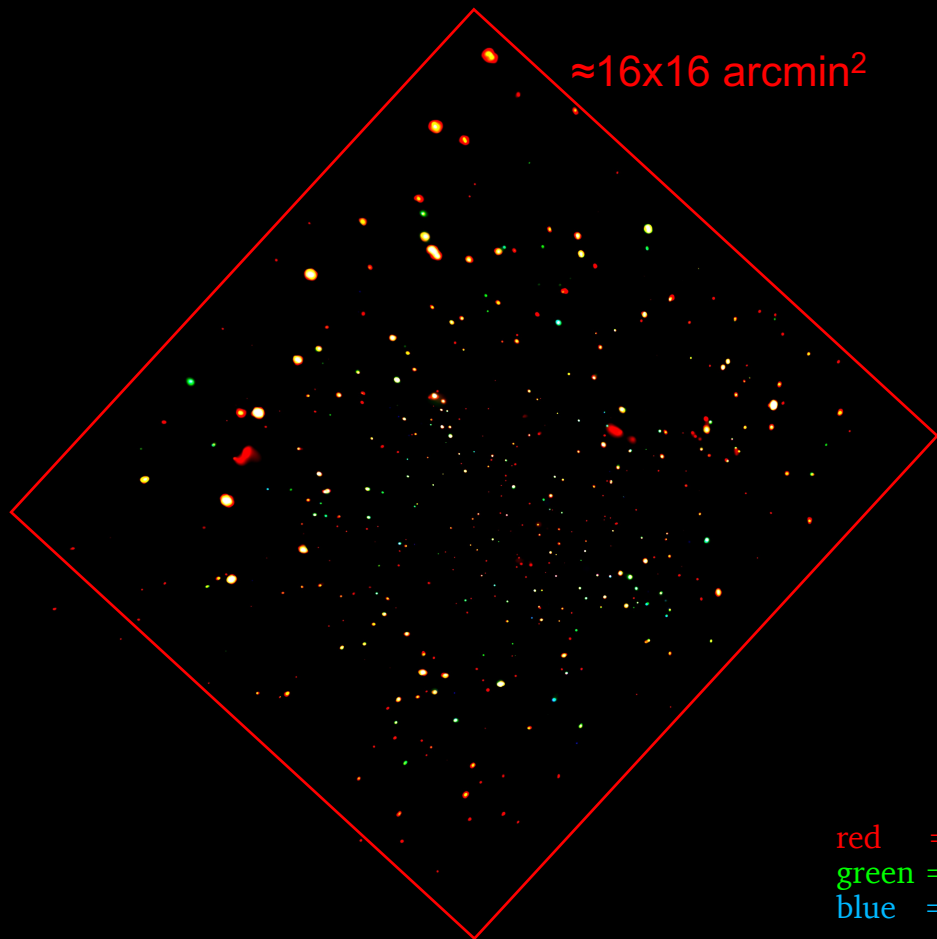
Table 1 continued

Survey name	Rep. Eff. Exp. (ks)	Solid angle (arcmin 2)	Representative reference
3XMM ^a	15	2,300,000	Watson (2012)
Stripe 82X– <i>XMM-Newton</i> ^a	15	37,800	LaMassa et al. (2013a)
XMM-LSS	10	39,960	Chiappetti et al. (2013)
XMM-XXL	10	180,000	Pierre (2012)
Stripe 82X– <i>XMM-Newton</i> Targeted	8	129,600	PI: C.M. Urry
<i>XMM-Newton</i> Slew Survey (XMMSL1) ^a	0.006	8×10^7	Warwick et al. (2012)
<i>NuSTAR</i> (3–24 keV)			
Extended CDF-S (E-CDF-S)	200	1,100	Mullaney et al., in prep
AEGIS-X	270	860	Aird et al., in prep
COSMOS	65	6,120	Civano et al., in prep
Serendipitous survey ^a	22	19,000	Alexander et al. (2013)

^a Serendipitous survey; see Sect. 2.1 for brief discussion regarding such surveys

Chandra Deep Fields

CDFN (Alexander+03; Luo+ 08)



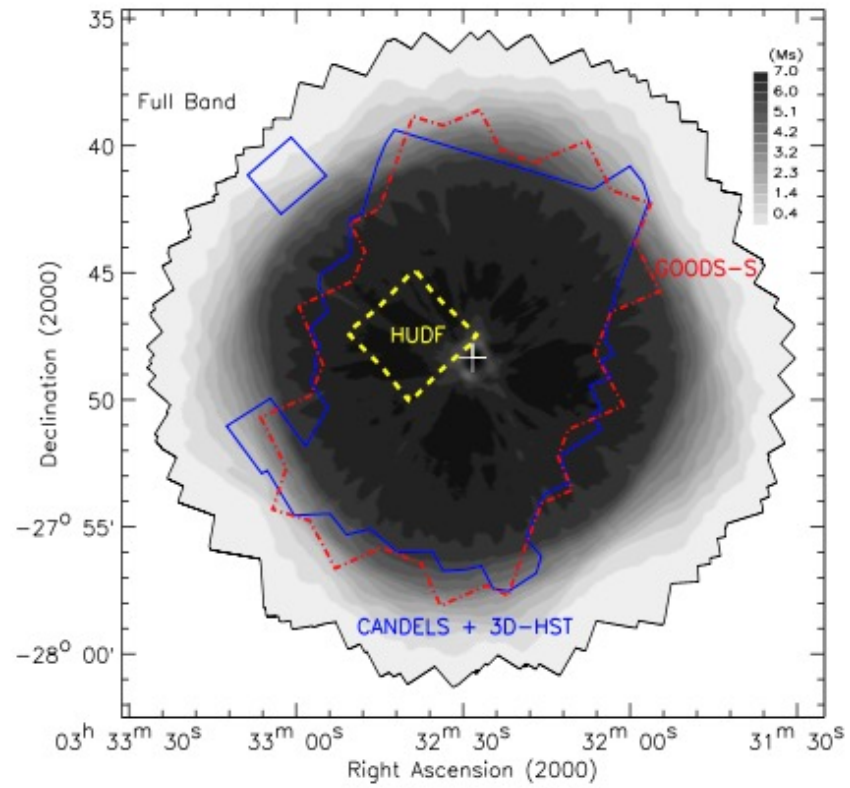
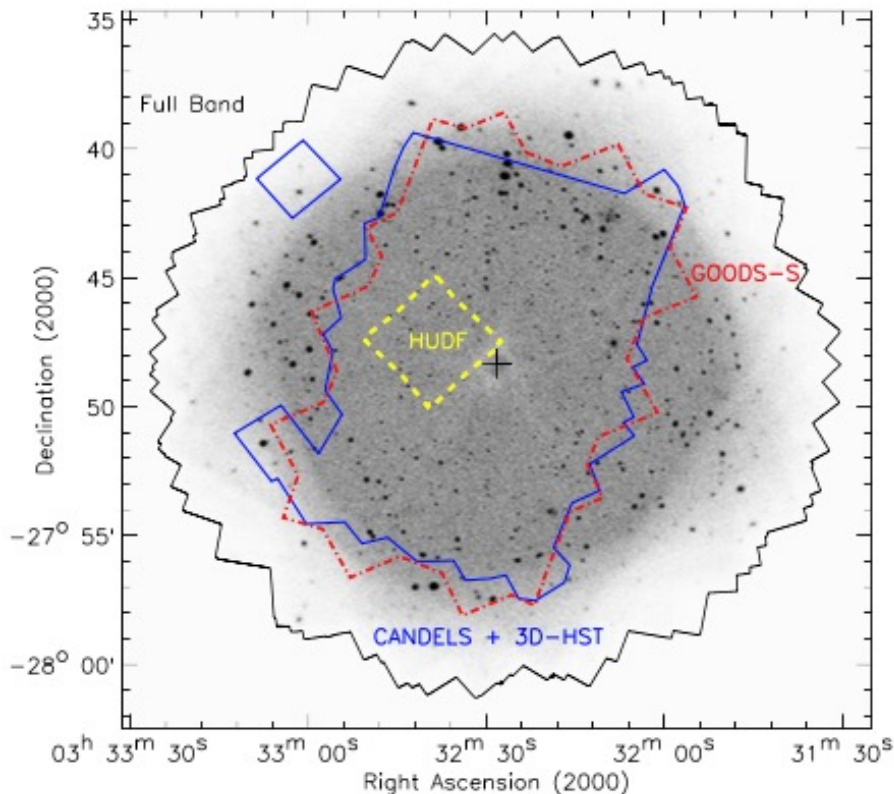
CDFS (Giacconi+02)



red = 0.5-1 keV
green = 1 - 2 keV
blue = 2 - 8 keV

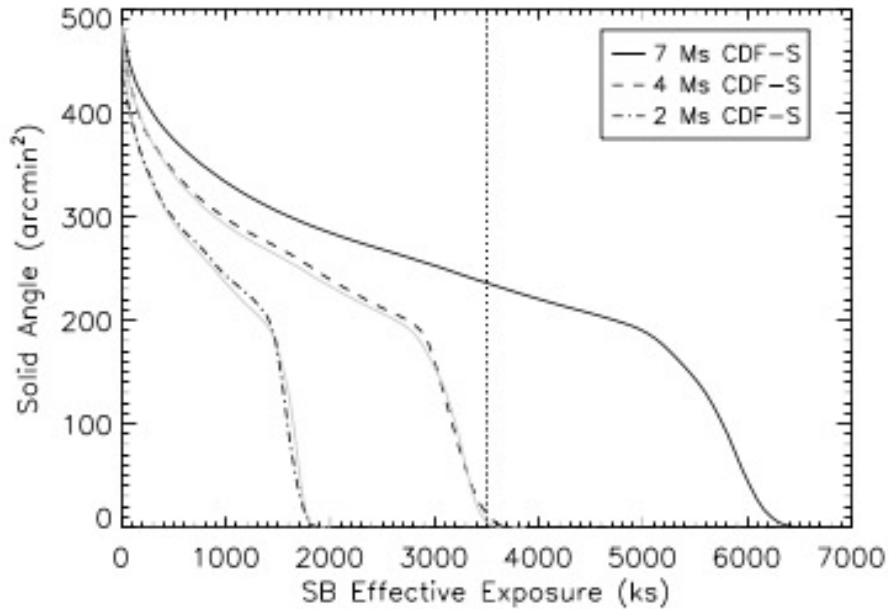
The 7Ms *Chandra* Deep Field South. I

The deepest X-ray exposure ever



- 484 arcmin²
- 1008 X-ray sources (992 with counterpart, ≈66% with spec. redshift)
- At least 70% are classified as AGN (the remaining are galaxies and stars)
- Inner 1 arcmin region: $F_{[0.5-7\text{keV}]} = 1.9 \times 10^{-17} \text{ erg/cm}^2/\text{s}$
 $F_{[0.5-2\text{keV}]} = 6.4 \times 10^{-18} \text{ erg/cm}^2/\text{s}$
 $F_{[2-7\text{keV}]} = 2.7 \times 10^{-17} \text{ erg/cm}^2/\text{s}$

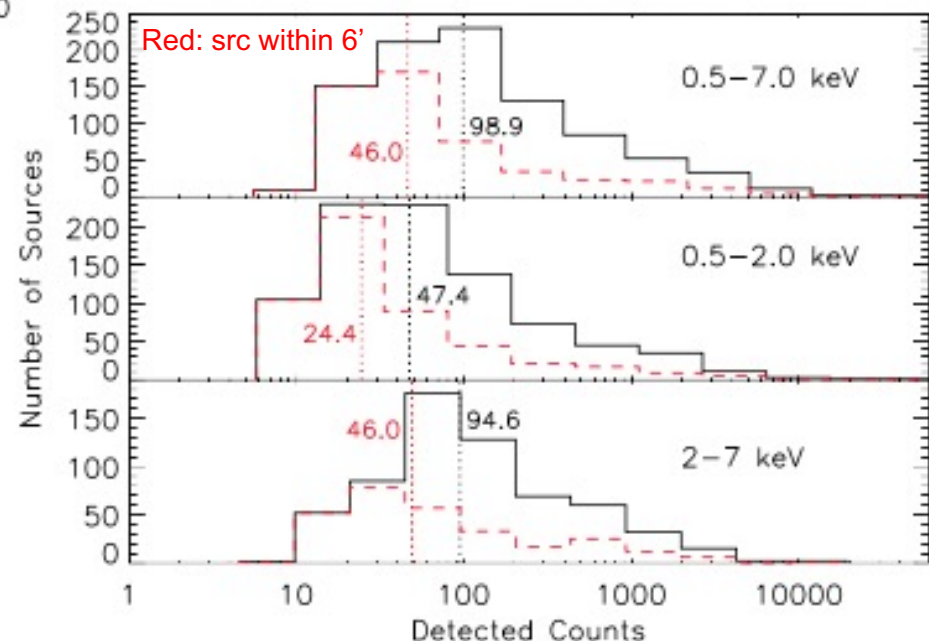
The 7Ms *Chandra* Deep Field South. II



Solid angle vs. exposure time
Motivations behind going deeper

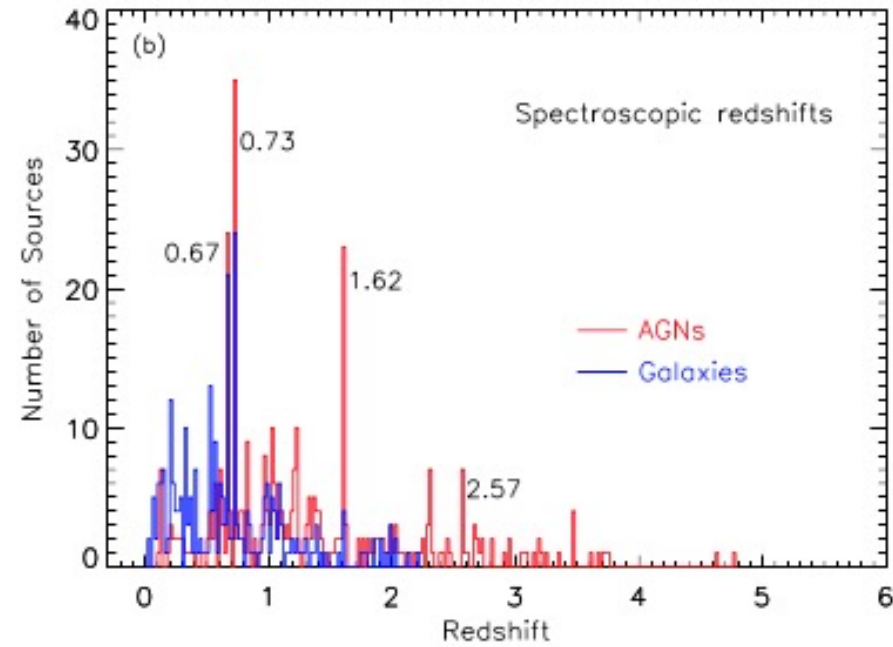
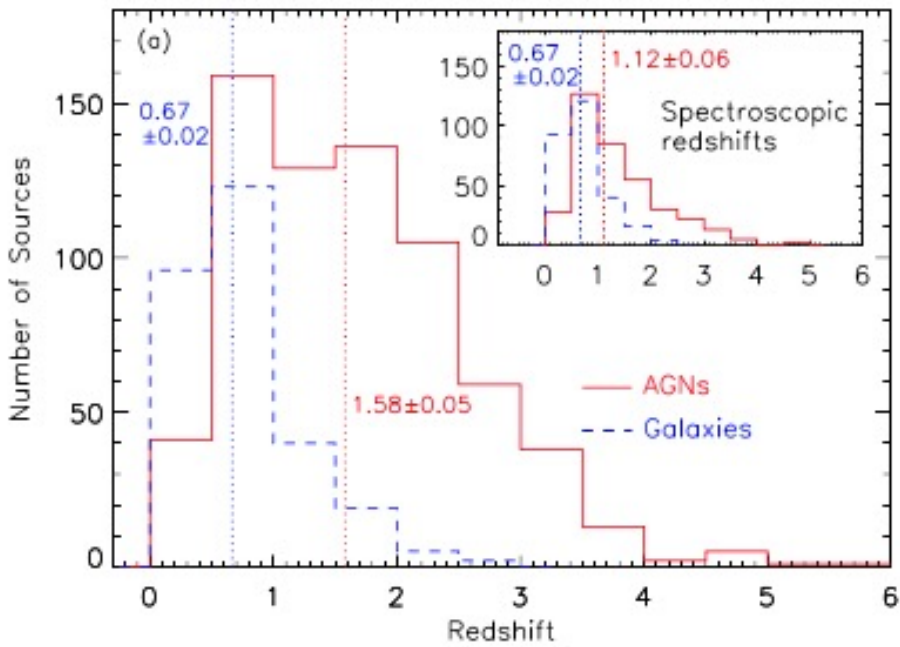
Number of counts
Median values around 100 (still low)

About 90% of the 0.5–2 keV XRB resolved into discrete sources in the CDF-S



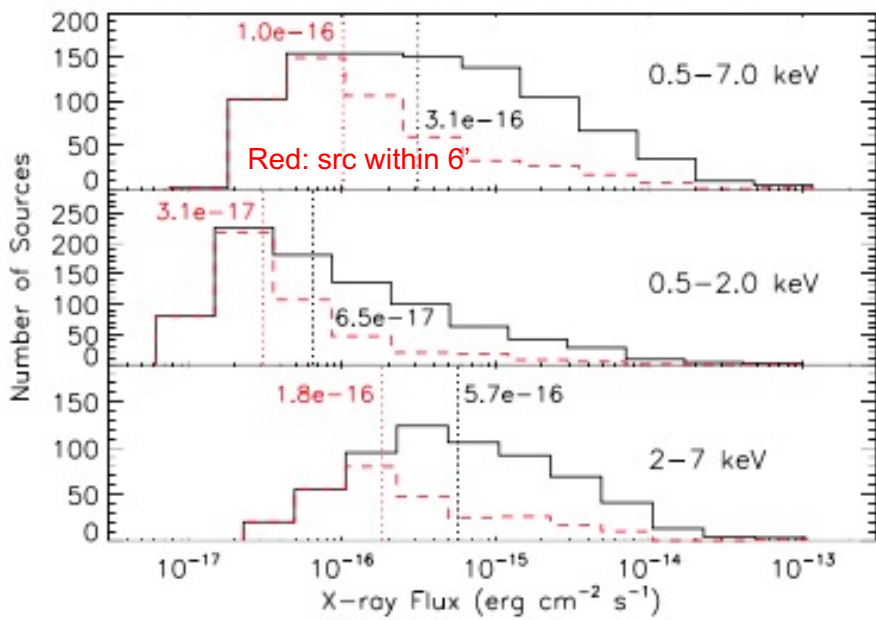
The 7Ms *Chandra* Deep Field South. III

Redshift distribution AGN vs. Galaxies



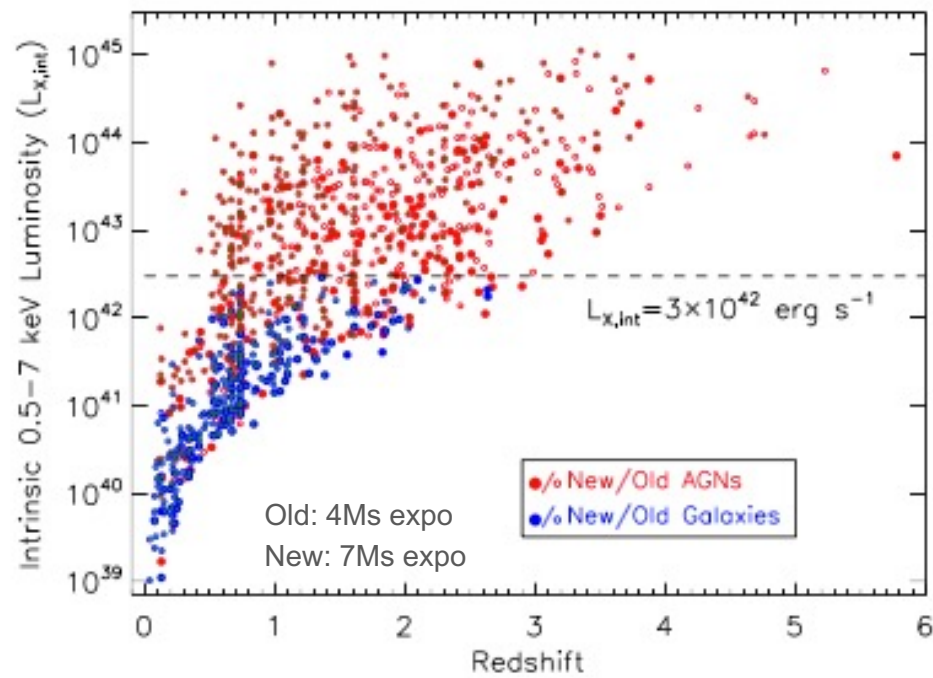
Luo+ 2017

The 7Ms *Chandra* Deep Field South. IV



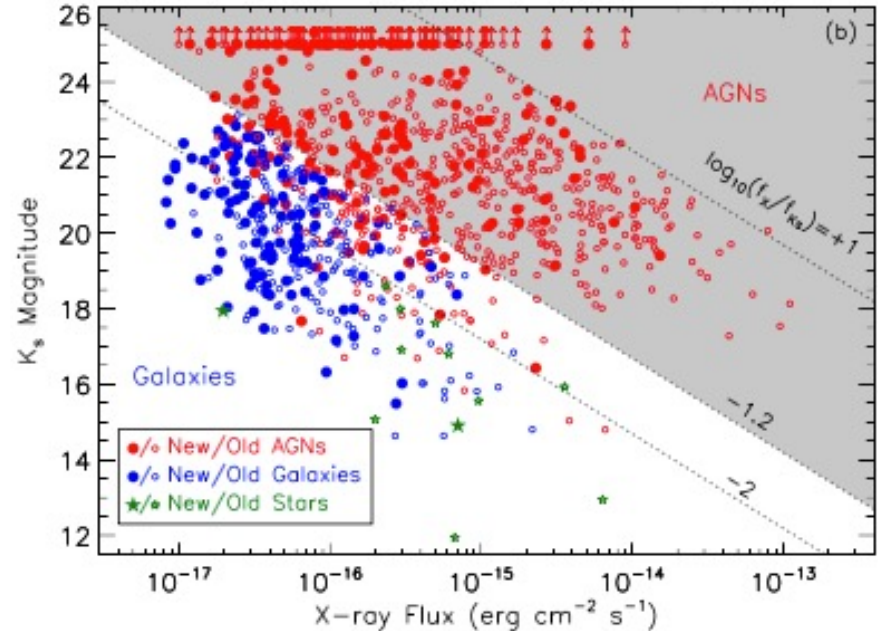
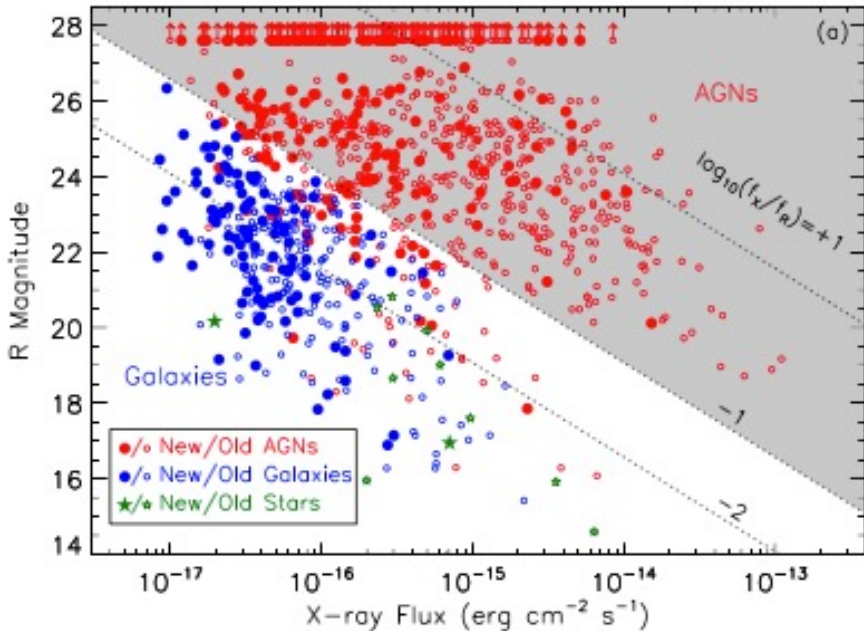
Flux distribution
Inner region vs. whole field

Luminosity distribution
AGN vs. Galaxies

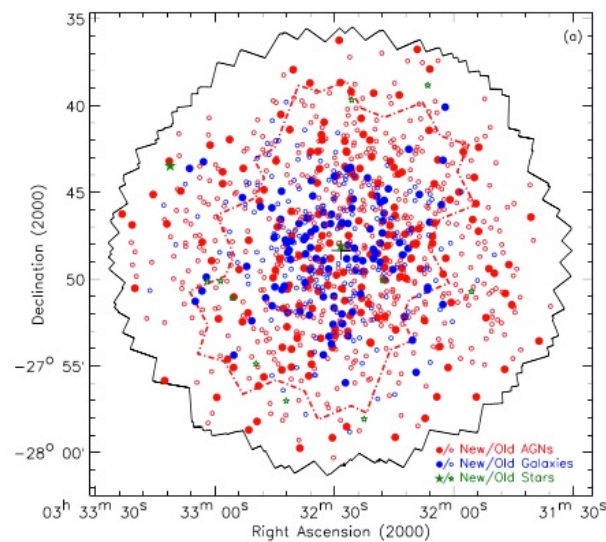


The 7Ms Chandra Deep Field South. V

R- (left panel) and K_s-band (right panel) mag vs. X-ray Flux



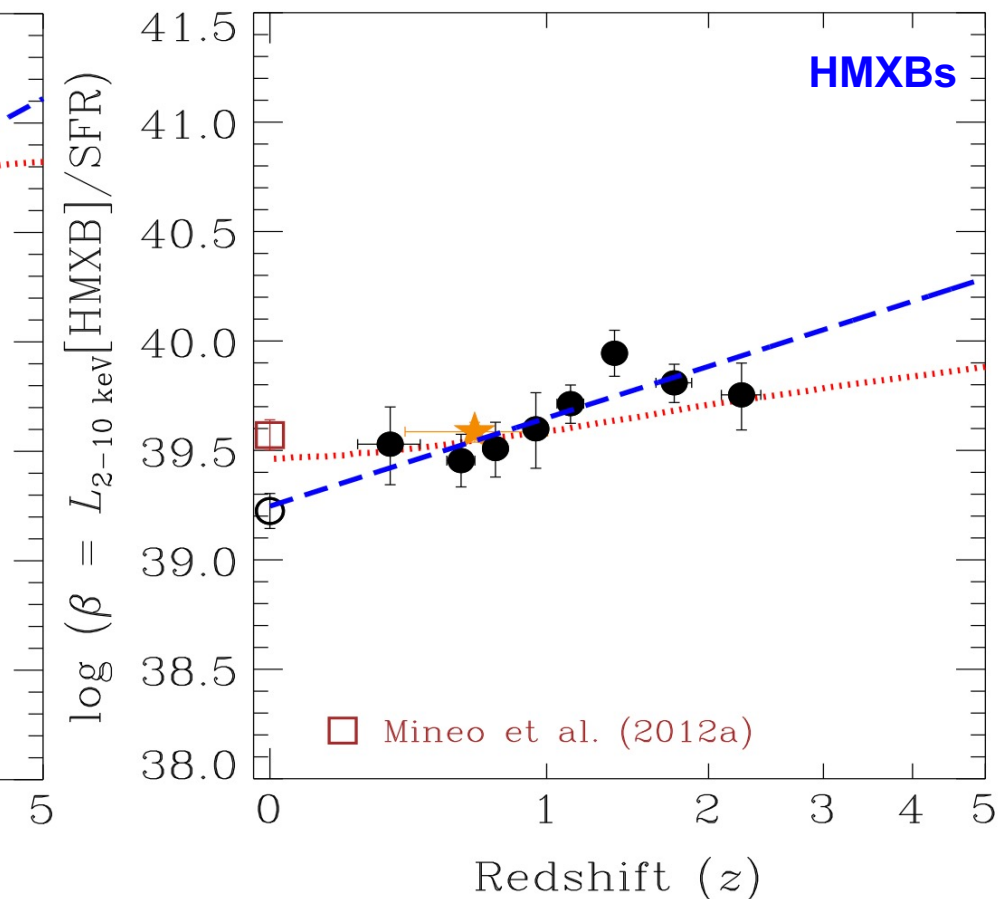
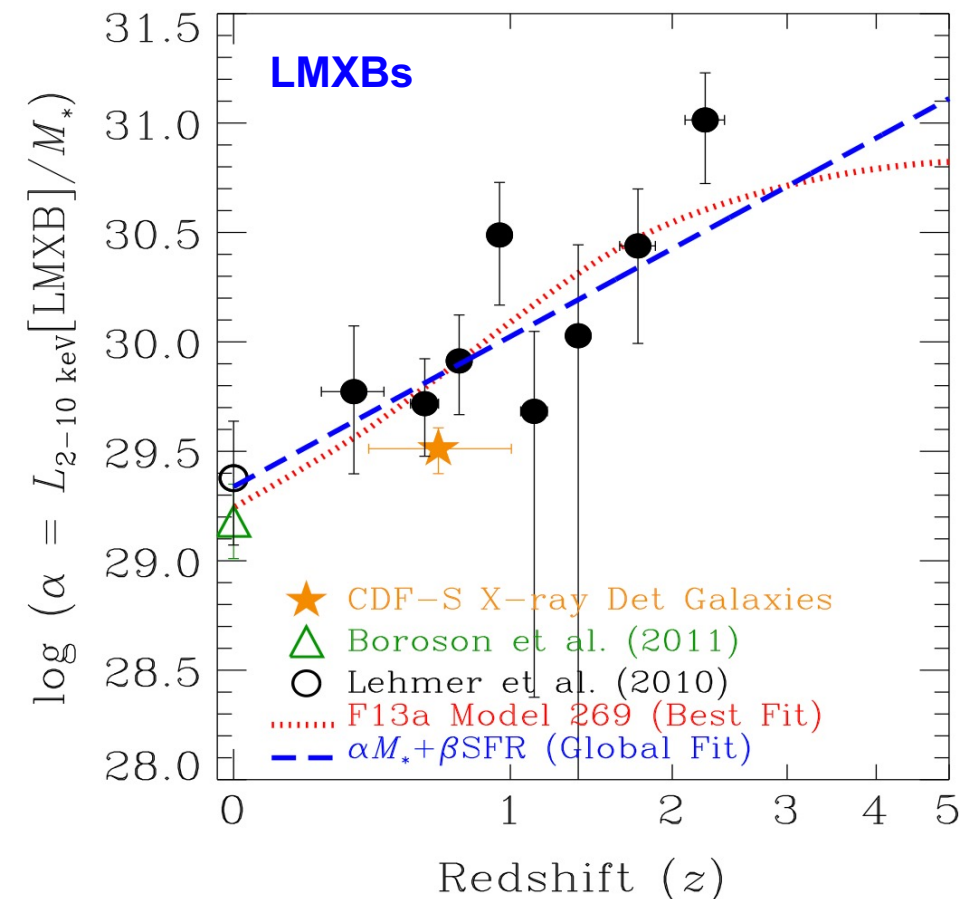
Luo+ 2017



Source statistics fundamental to populate
luminosity and redshift bins and study AGN
evolution and demographics

The 7Ms *Chandra* Deep Field South. VI

Brandt & Yang (2021, review)



Probing the populations of X-ray binaries through X-rays
 [Low-mass X-ray Binaries (LMXBs), High-mass X-ray binaries (HMXBs)],
 up to high redshifts (very deep exposures are needed → CDFS)

What about X-ray variability?

~17 yrs of observations

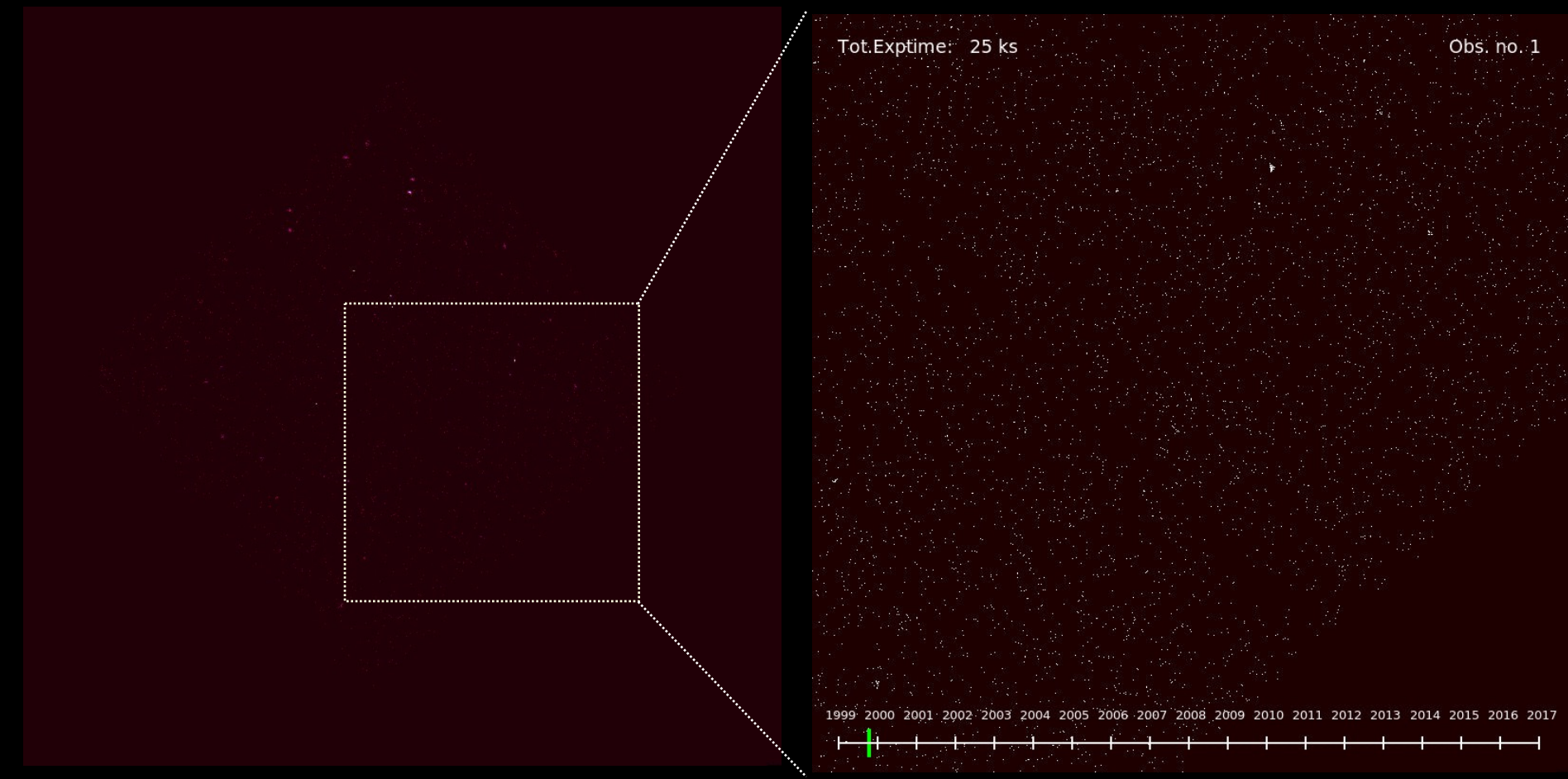
7Ms exposure
[4 chunks of obs]

Courtesy of Yang G.

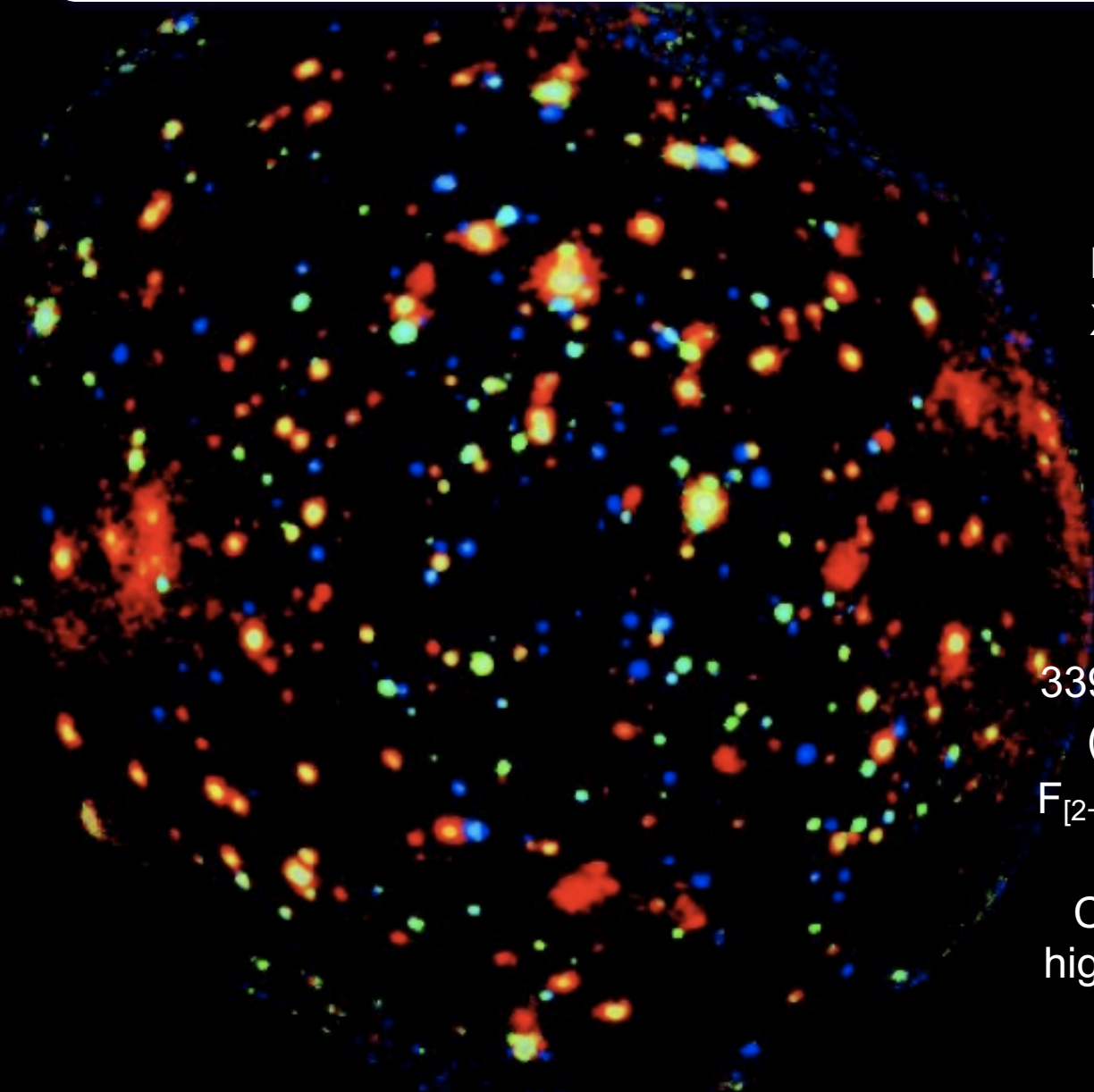
7Ms exposure
[4 chunks of obs, zoom]

Courtesy of Yang G.

Courtesy of M. Paolillo



Chandra Deep Field South: XMM 3 Ms exposure

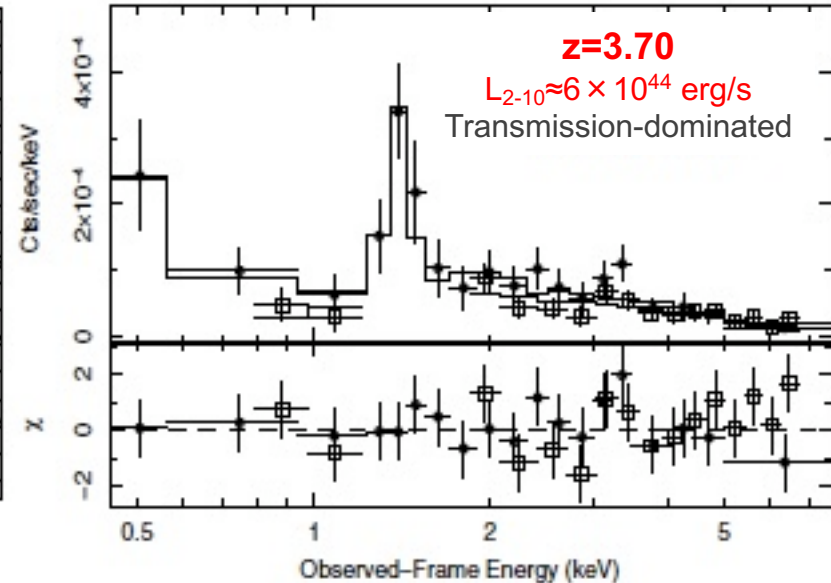
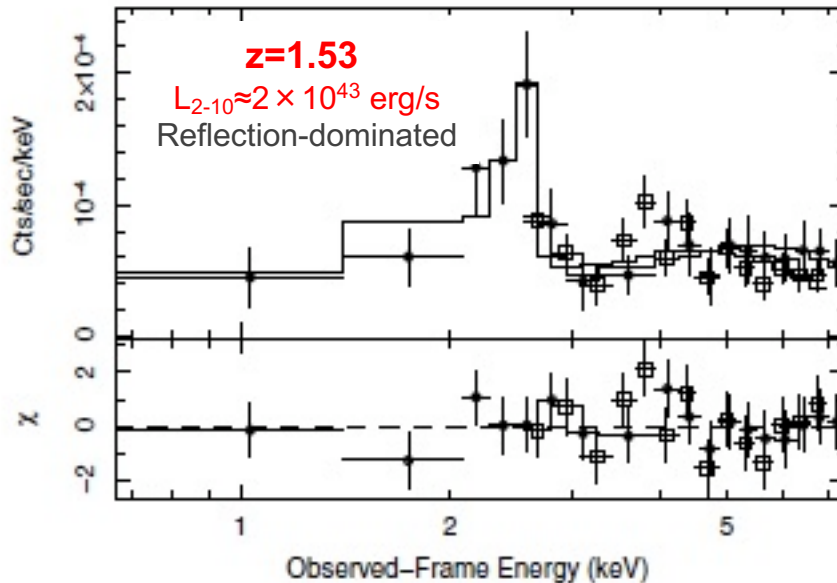


Larger field-of-view than Chandra, larger effective area, worst PSF, higher background → good for X-ray spectral analysis of relatively X-ray bright sources

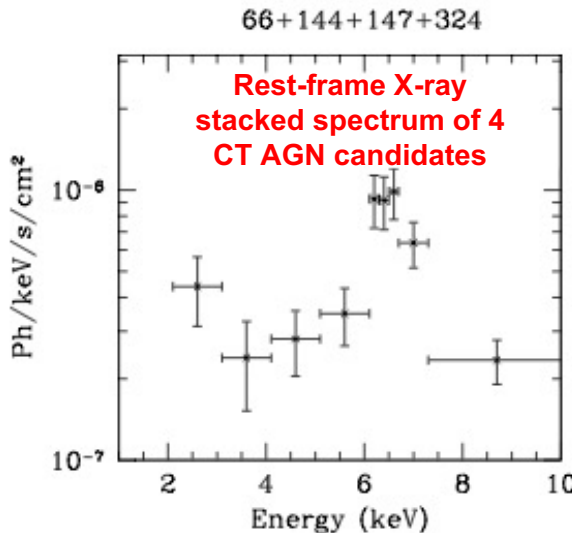
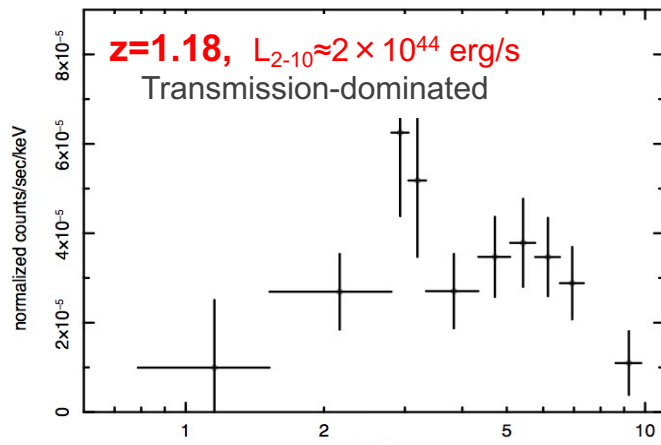
≈900 arcmin²
339 hard (2–10 keV) sources
(95% with spec/photo-z)
 $F_{[2-10\text{keV}]} = 6.6 \times 10^{-16} \text{ erg/cm}^2/\text{s}$

Capable of probing the high-z Universe with good photon statistics

The 3 Ms XMM-Newton Survey in the CDF-S. I

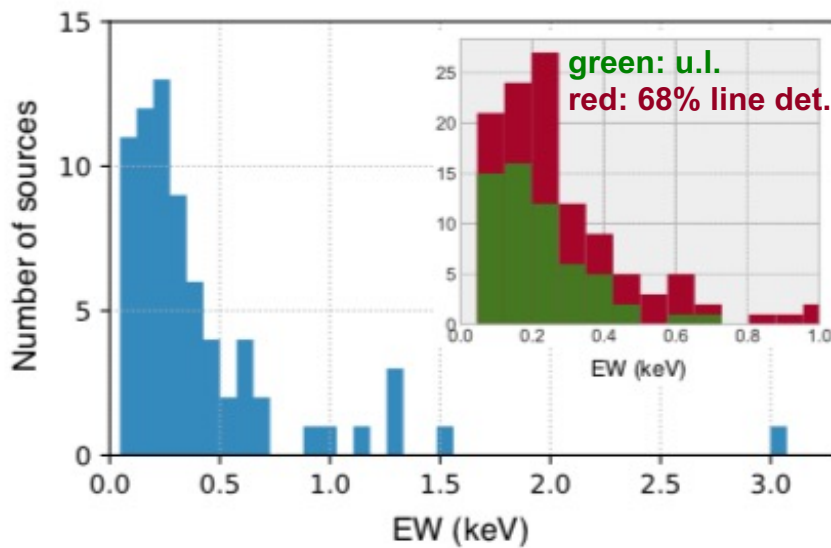


Comastri et al. (2011); see also Iwasawa et al. (2020)

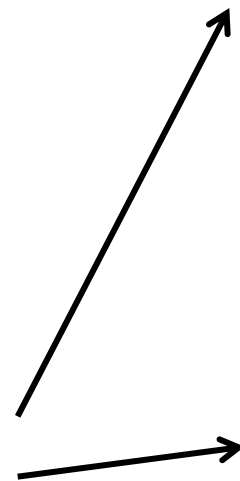


The 3 Ms XMM-Newton Survey in the CDF-S. II

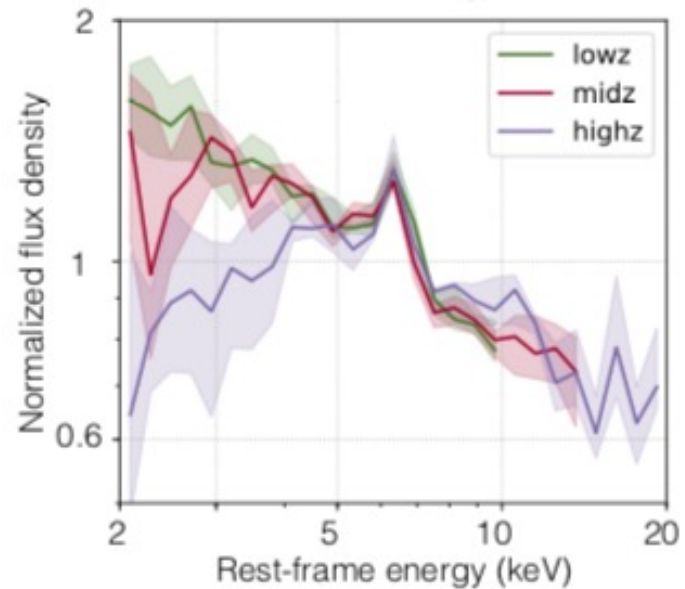
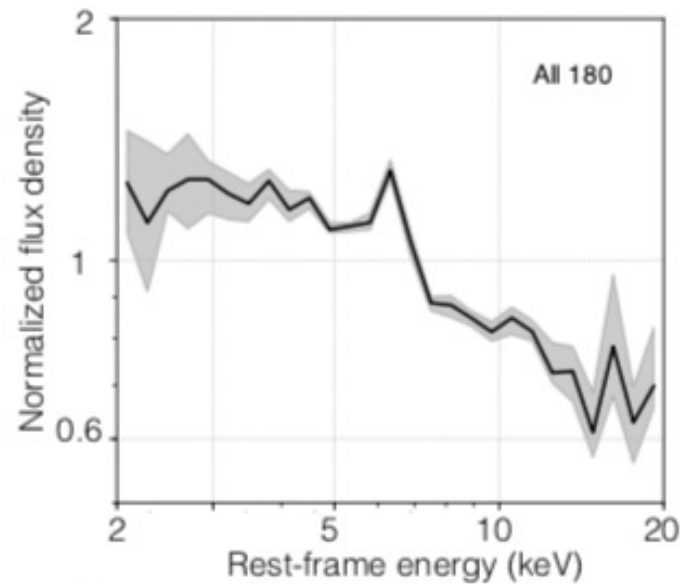
iron K α EW analysis → search for obscured AGN



composite spectra:
180 X-ray sources at $z=0.4-3.8$

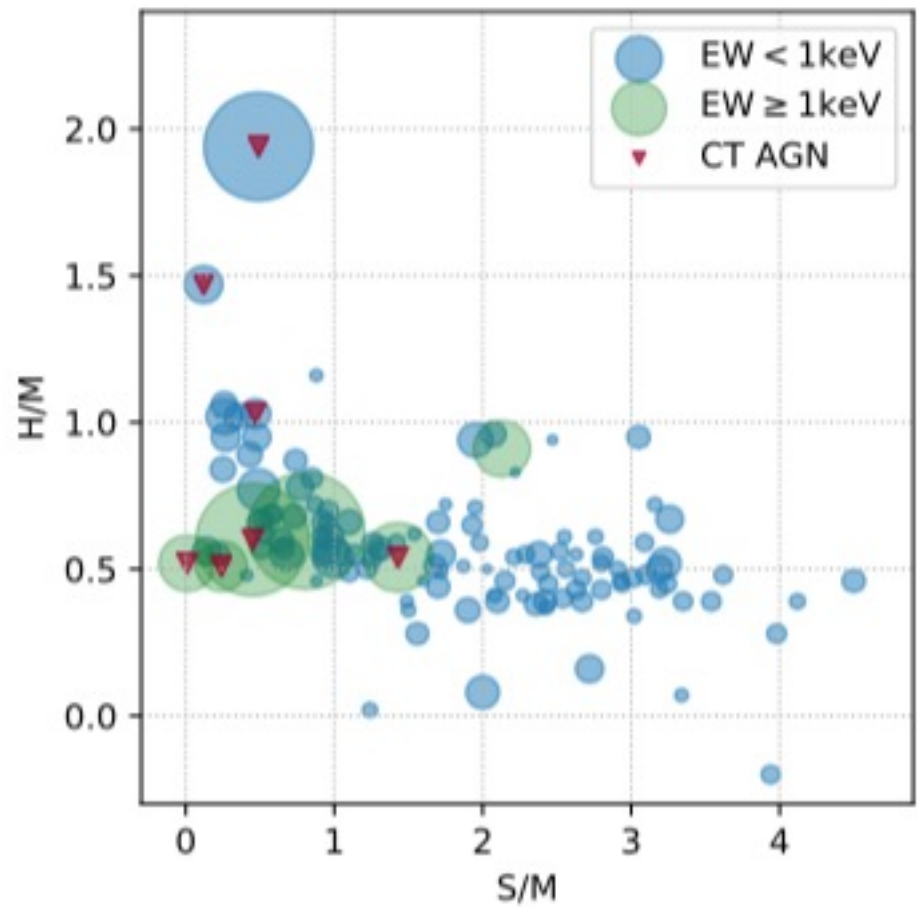
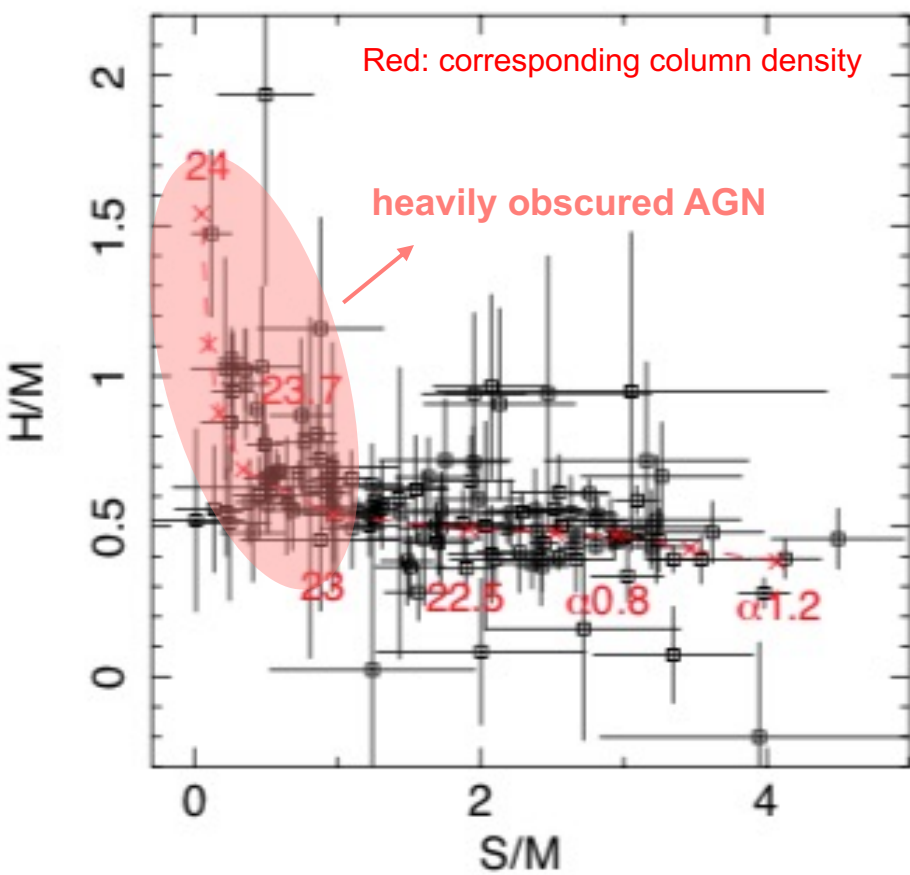


Iwasawa et al. (2020)



The 3 Ms XMM-Newton Survey in the CDF-S. III

combining hardness ratio (HR) or band ratio and iron K α EW analysis to pick up obscured sources



'hardness' ratio (here: band ratio) selection to pick up very obscured AGN.

This is generally confirmed by high EW of the iron line

S=2–5 keV rest frame
M=5–9 keV rest frame
H=9–14 keV rest frame

Iwasawa et al. (2020)

X-raying the COSMOS

XMM-Newton

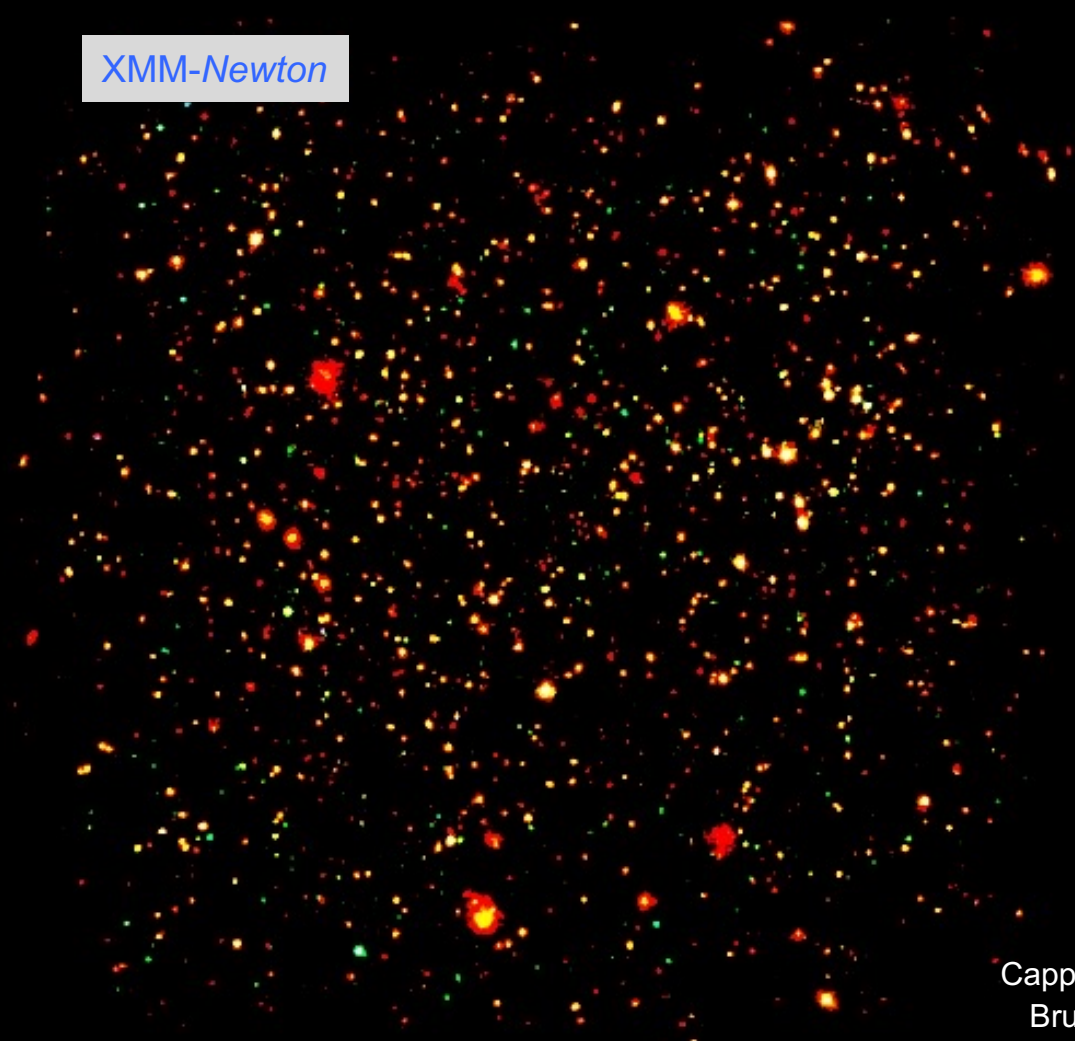
1.55 Ms

1822 sources

Large area, 2 deg², good
photon statistics

Background and PSF size
main limitations

XMM-Newton



Cappelluti+09
Brusa+10

X-raying the COSMOS

The final **COSMOS-Legacy** Field

XMM-Newton

1.55 Ms

1822 sources

Large area, 2 deg^2 , good
photon statistics

Background and PSF size
main limitations



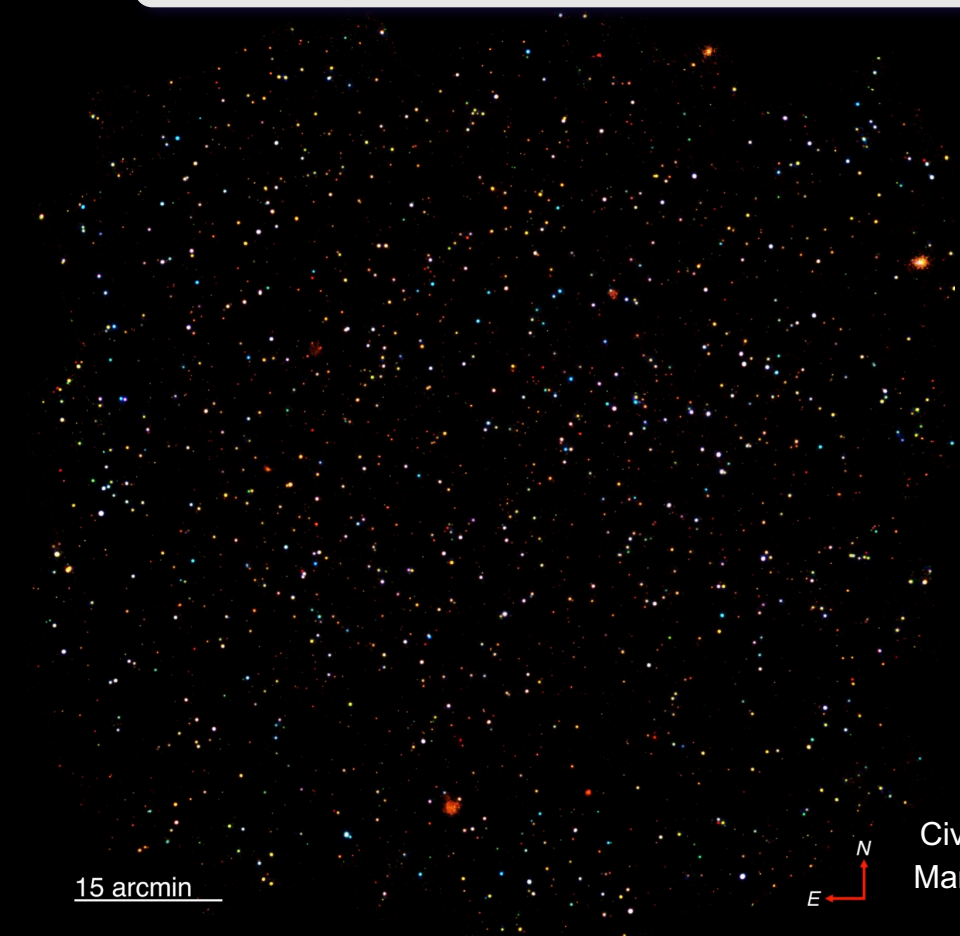
Chandra

4.6 Ms

2.2 deg^2

150 ks uniform

4016 sources



Chandra

AGN Evolution from (X-ray) surveys

AGN luminosity function: basic definition

The space density of sources of different intrinsic luminosities, L , is described by the *luminosity function* (LF), $\phi(L)$, so that $dN = \phi(L)dL$ is the number of sources per unit volume with luminosity in the range L to $L + dL$. Let us consider, for simplicity, the local or nearby (Euclidean) universe uniformly filled with sources with LF $\phi(L)$. If S is the limiting flux that we can detect, sources with luminosity L can be observed out to a distance $r = (L/4\pi S)^{1/2}$. The number of sources over the solid angle Ω , observable down to the flux S are:

$$N(> S) = \int \frac{\Omega}{3} r^3 \phi(L) dL = \frac{\Omega}{3(4\pi)^{3/2}} S^{-3/2} \int L^{3/2} \phi(L) dL. \quad (1)$$

Thus, independent of the exact *shape* of the luminosity function entering in the determination of a normalization constant, the *slope* of the cumulative number counts of any non-evolving class of sources in a uniform, Euclidean universe should always be equal to $d \log N(> S) / d \log S = -3/2$ (if we use magnitudes, m , instead of luminosities, then $d \log N(> m) / dm = 0.6$).

$$\phi(L, z) = f_d(z) \phi(L/f_l(z), z = 0). \quad (2)$$

In the *pure luminosity evolution (PLE)* case ($f_d = \text{const.}$), the co-moving number density of sources is constant, but luminosity varies with cosmic epoch; in the *pure density evolution (PDE)* case ($f_l = \text{const.}$), but the co-moving density of sources of any luminosity varies.

AGN luminosity functions

★ luminosity evolution $L_\star = L_\star(z)$

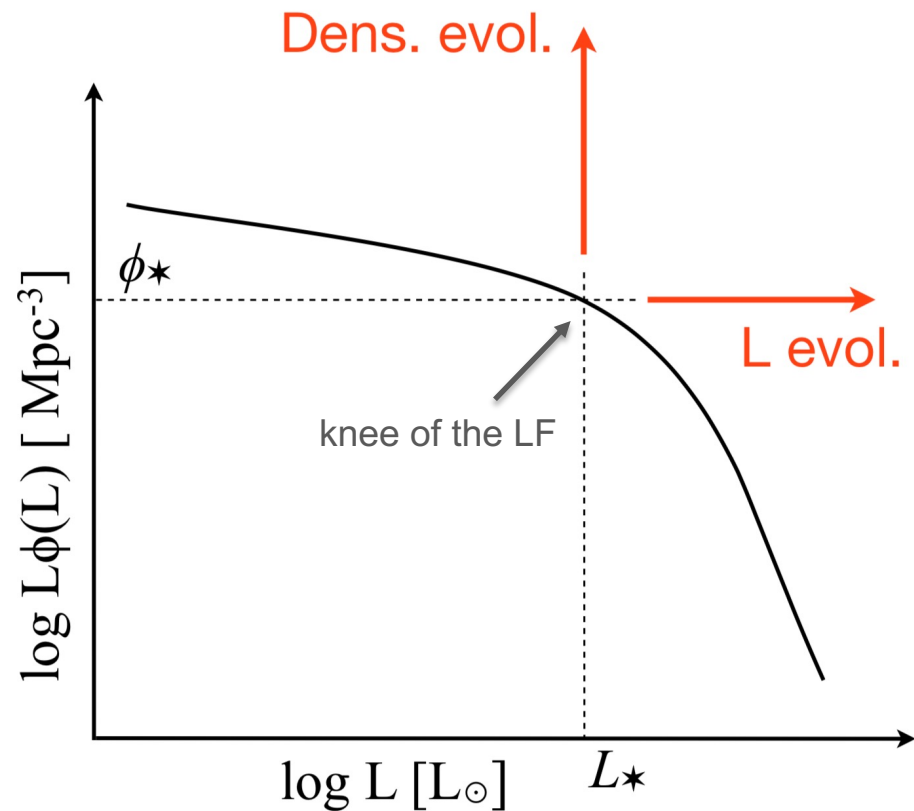
$$\phi(L, z) = \phi\left(\frac{L}{L_\star(z)}, 0\right)$$

★ density evolution

$$\phi(L, z) = n(z)\phi(L, 0)$$

★ luminosity-density evolution

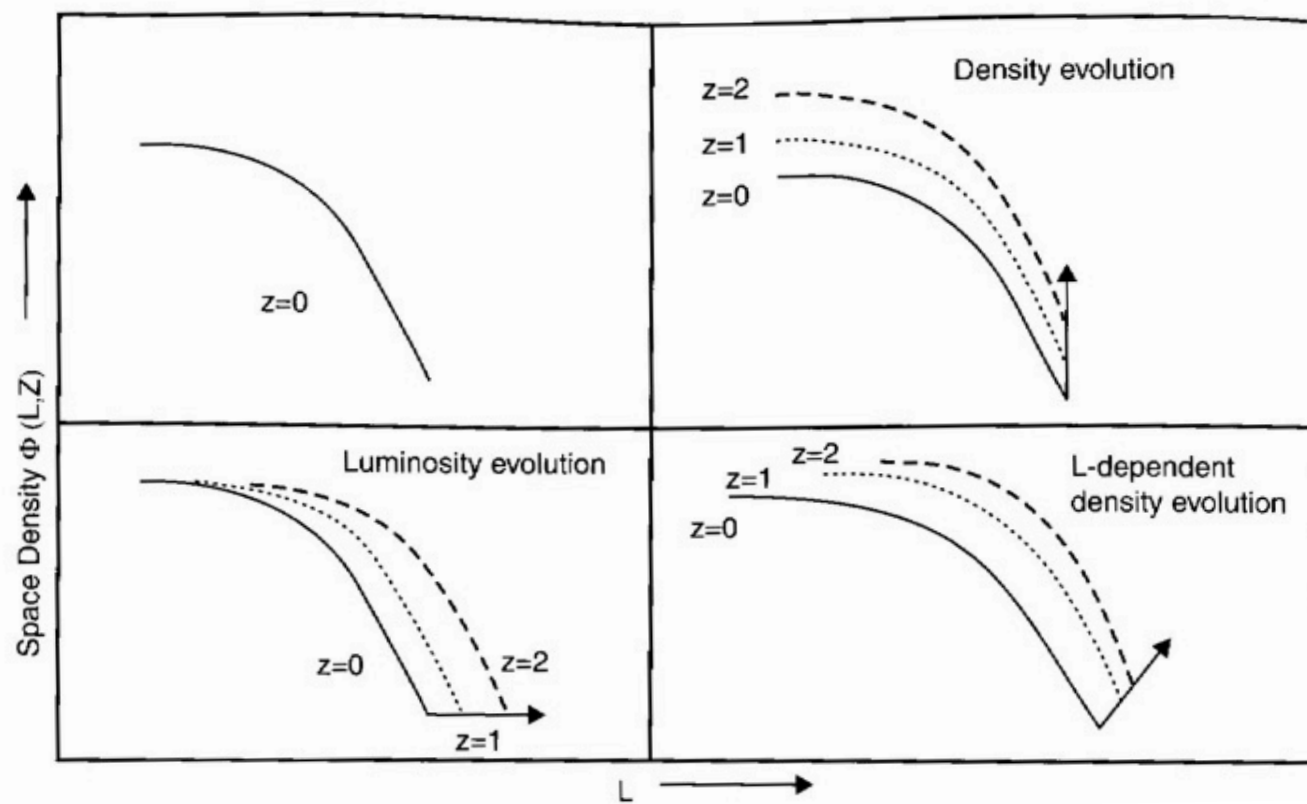
$$\phi(L, z) = n(z)\phi\left(\frac{L}{L_\star(z)}, 0\right)$$



Luminosity Evolution:
AGN more luminous in the past

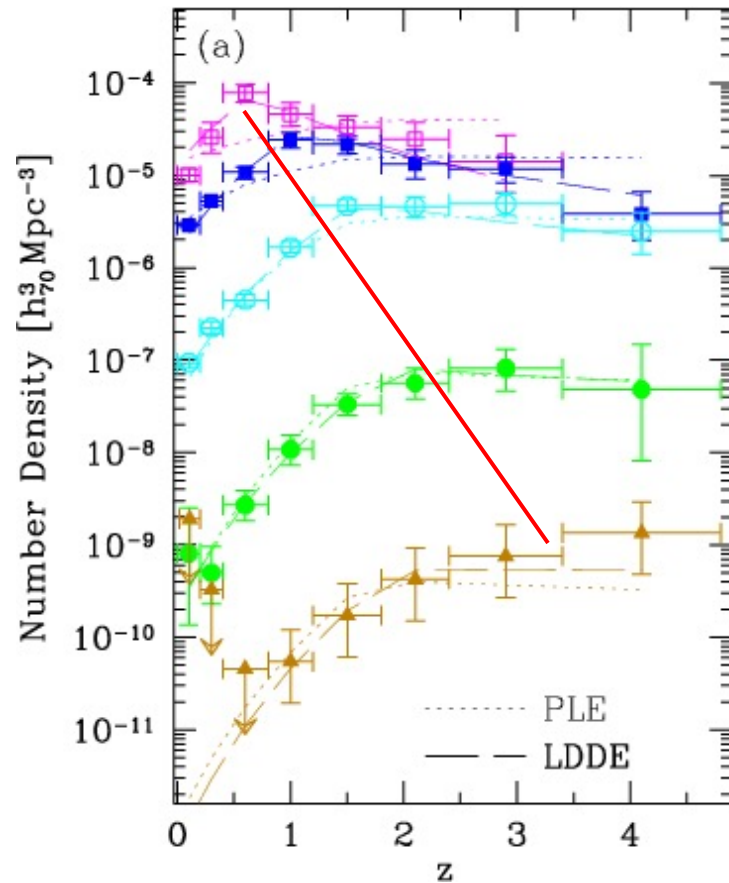
Density Evolution:
AGN more numerous in the past

Luminosity-dependent Density Evolution:
Evolution in density dependent on AGN luminosity

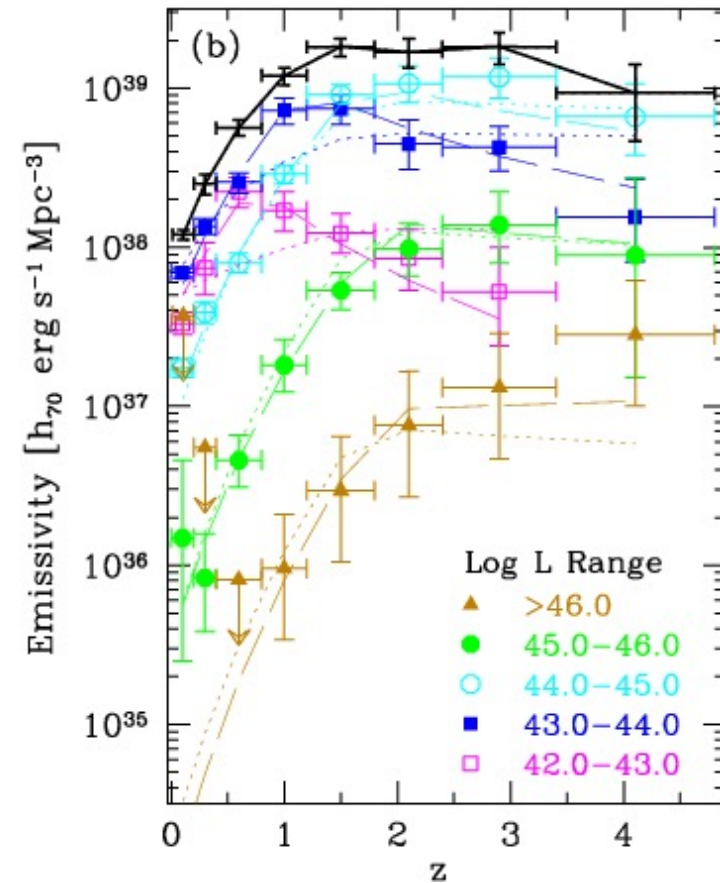


AGN cosmological evolution. I

Number density



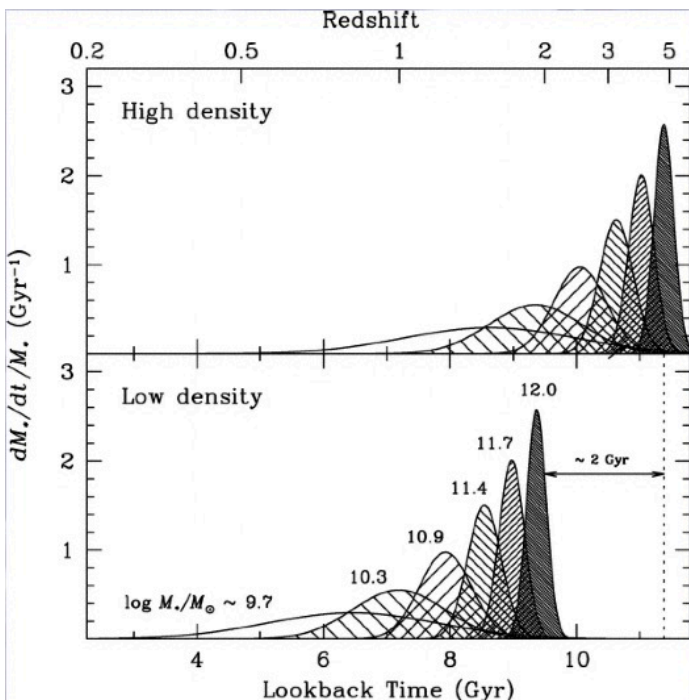
Luminosity density



Objects with lower luminosity peak at lower redshift, similar to what observed for SFR in galaxies \Rightarrow **cosmic downsizing**
QSOs peak at $z \approx 2-3$, AGN at $z \approx 0.5-1$

AGN cosmological evolution. II

- The number density of AGN evolves differently for sources of varying luminosities → LDDE (luminosity-dependent density evolution) is the current, widely accepted parameterization of AGN evolution in X-rays
- The density of the most luminous AGN peaks earlier in cosmic time than for less luminous objects, which likely implies that large black holes are formed earlier than their low-mass counterparts
- Similar behavior for galaxies: massive galaxies tend to form stars earlier and faster than less massive galaxies (*downsizing*, Cowie+96)

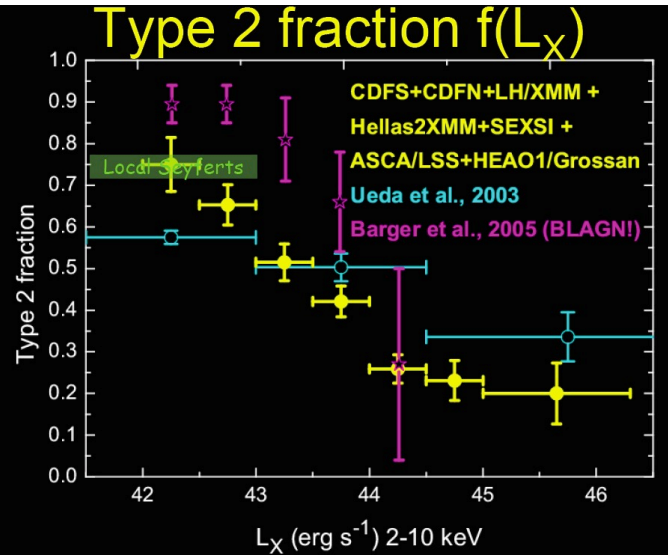


Galaxy formation took place in “downsizing”, with more massive galaxies forming at higher redshift
(Cowie+96)

AGN and galaxies seem to share a similar behavior in terms of evolution

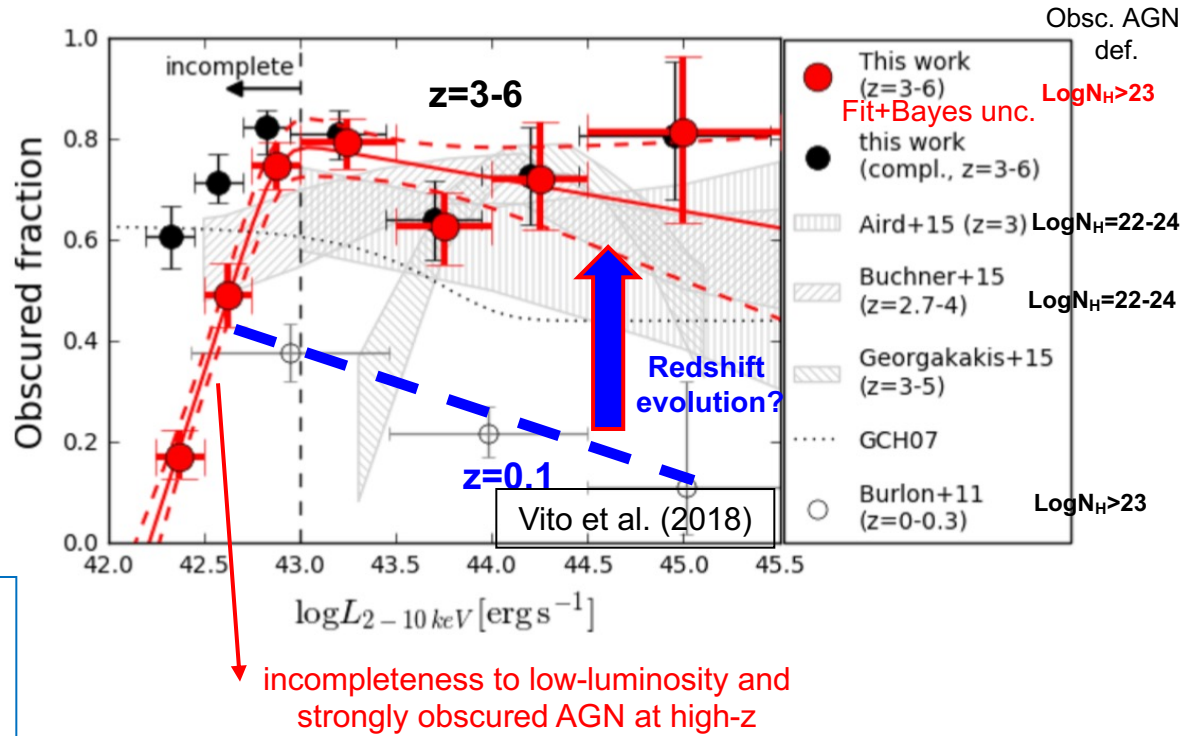
Thomas+2005

Dependence of the obscured AGN fraction on X-ray luminosity and redshift



Broad consensus for an obscured AGN fraction declining towards high intrinsic luminosities, consistently with the **receding torus model** (Lawrence 1991, Simpson 2005; see also Lusso et al. 2013)

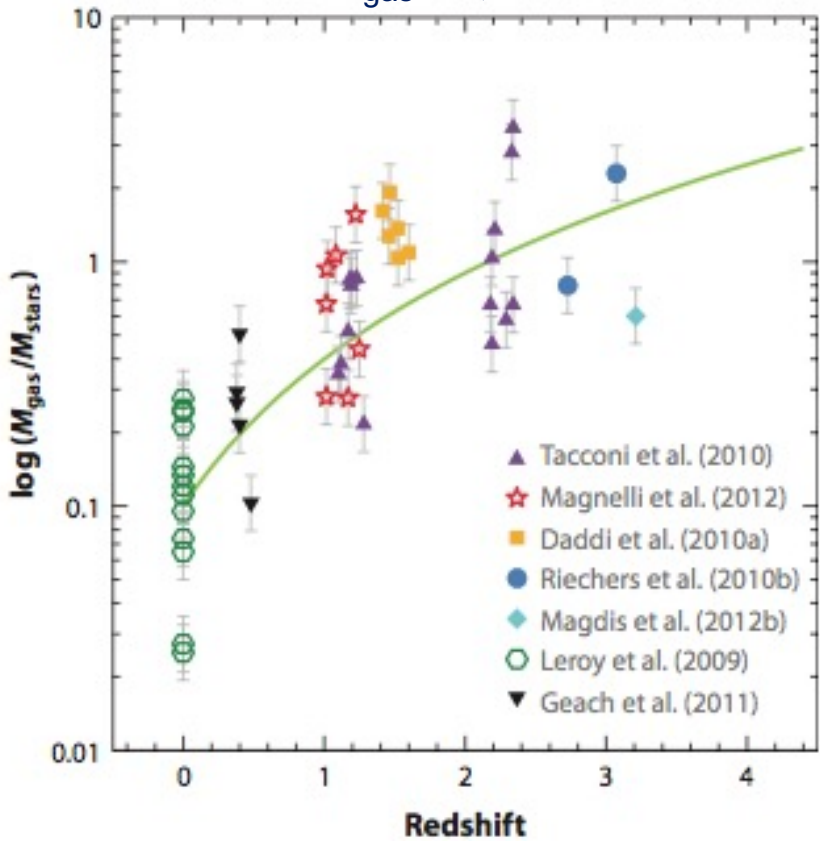
Behavior with z still debated (see e.g. La Franca et al. 2005; Treister & Urry 2009; Iwasawa et al. 2012; Vito et al. 2013, 2014, Buchner et al. 2015; likely increasing with z)



$z>3$ AGN: $\approx 70-80\%$ with $N_H>10^{23} \text{ cm}^{-2}$
see also Iwasawa et al. (2012) – CDFS, 3Ms, $z=1.7-3.7$

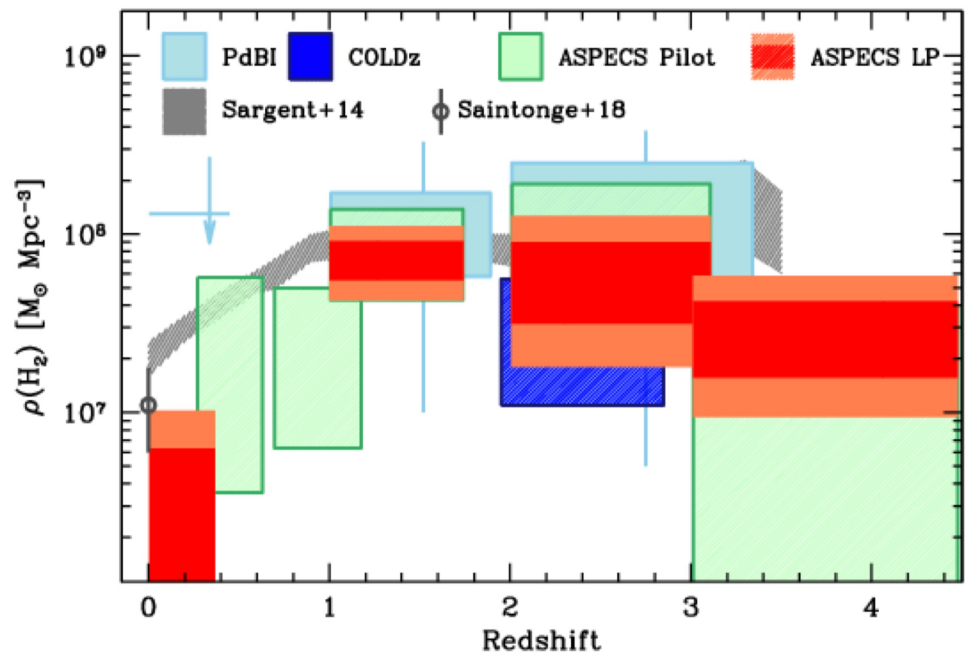
Obscured AGN fraction increases with redshift, especially at high luminosity
More gas available, more mergers, ...
(More on this issue in the high- z AGN lesson)

M_{gas}/M_{\star} vs. Z



Carilli & Walter (2013)

ρ_{gas} vs. Z



Decarli et al. (2019)

- Large quantity of gas available at high redshift
- Higher merger rate and more gas available for the accreting SMBHs at high redshift; larger covering factors? The same gas sustaining strong SF at high redshift may be responsible for the obscuration – more on high-z AGN lesson

The Soltan argument. I

Soltan (1982) estimated of the **BH mass density in the Universe** ρ_{BH} which should exist in the local Universe as ‘dead quasars’.

This method consists of summing all the energy emitted by active SMBHs since the formation of the first objects and ‘converting’ the total bolometric luminosity integrated over the entire cosmic history into the total SMBH mass at $z=0 \rightarrow$ **the mass in black holes today is simply related to the AGN population integrated over luminosity and redshift (i.e., the AGN LF)**

It is a sort of ‘photon-counting exercise’: *every photon radiated by an active BH during the history of the Universe represents a certain amount of grams of SMBH mass today*

Assumption: all accretion onto SMBHs leads to radiation: $L = L_{\text{bol}} = \eta \dot{M} c^2$

$$u = \int_z^\infty \frac{dt}{dz} dz \int_0^\infty \Phi(L, z) \text{AGN LF} L dL \quad \begin{matrix} \text{Integrated} \\ \text{energy} \\ \text{density from} \\ \text{all AGN} \end{matrix}$$

$$\rho_{\text{BH}} = \int_z^\infty \frac{dt}{dz} dz \int_0^\infty \Phi(L, z) \frac{1-\eta}{\eta c^2} L dL \quad \begin{matrix} \text{Mass density} \\ \text{of SMBH} \\ \text{‘remnants’} \\ \text{see also lesson 1} \end{matrix}$$

The Soltan argument. II – Description of the steps

- BH growth rate for an AGN with luminosity L

$$L = \eta \dot{M}_{acc} c^2$$

$$\dot{M}_{BH} = (1 - \eta) \dot{M}_{acc} = \frac{1 - \eta}{\eta c^2} L$$

$$\Phi(L, z) \; dL$$

Number per unit volume of AGN in L, L+dL @z

$$\dot{M}_{BH}(L) \; \Phi(L, z) \; dL$$

BH growth rate per unite volume for AGN in L, L+dL @z

$$\dot{M}_{BH}(L) \; \Phi(L, z) \; dL \left| \frac{dt}{dz} \right| dz$$

BH mass per unit volume accreted from AGN emitting L, L+dL during cosmic time z, z+dz

- The remnant BH mass density is then obtained by integrating for L and z for all AGN at all cosmic times

$$\rho_{BH} = \int_0^\infty dz \int_0^\infty dL \left(\frac{1 - \eta}{\eta c^2} L \right) \Phi(L, z) \; dL \left| \frac{dt}{dz} \right| dz$$

The Soltan argument. III – Description of the steps

- The integrated comoving energy density from AGN/quasars is

$$u = \int_0^\infty dz \int_0^\infty dL \Phi(L, z) L \left| \frac{dt}{dz} \right|$$

$$\Phi(L, z) dL$$

Number of AGN (quasars) per unit volume for AGN in L , $L+dL$ @ z

$$L \Phi(L, z) dL$$

Luminosity density of AGN in L , $L+dL$ @ z

$$\Phi(L, z) dL dt$$

Energy density of AGN in L , $L+dL$ radiated in z , $z+dz$

- The expected remnant mass density is

$$\rho_u = \frac{1 - \eta}{\eta c^2} u$$

The Soltan argument. IV

- Soltan (1982) used the quasar luminosity function in the B-band to obtain the bolometric luminosity function (using a bolometric correction k_{bol} : $L \sim 10 v_B L_{v,B}$)

$$\Phi(L_B, z) dL_B = \Phi(L, z) dL$$

- Integrated comoving energy density from quasars (Soltan 1982)

$$u = \int_0^\infty dz \int_0^\infty dL \Phi(L, z) L \left| \frac{dt}{dz} \right| \sim 1.3 \times 10^{-15} \text{ erg cm}^{-3}$$

$$\rho_u = \frac{1 - \eta}{\eta c^2} u \sim 2.2 \times 10^5 M_\odot \text{ Mpc}^{-3} \quad \text{assuming } \eta=0.1$$

- Local mass density $\sim (3.5 - 5.5) \times 10^5 M_\odot \text{ Mpc}^{-3}$ (see Yu & Tremaine 2002, Marconi et al. 2004, Shankar et al. 2008)
- Sources of uncertainties: (a) AGN are not only Type 1 as in Soltan (1982) description → first optical quasar survey picked up mostly unobscured AGN and (b) the ‘matter-energy conversion’ efficiency might be $\neq 10\%$ (assumed by Soltan)

The Soltan argument and the SMBH accretion history information ‘stored’ in the XRB. I

- The XRB records the accretion history onto SMBHs across cosmic time (i.e., is the integrated emission of AGN and quasars at all luminosities and redshifts).
The XRB intensity at energy E is given by

$$I(E) = \frac{1}{4\pi} \int_0^{z_{max}} \int_0^{\infty} \frac{(1+z)f[E(1+z)L_X]}{4\pi D_L^2} \Phi(L_X, z) dL_X \frac{dV}{dz} dz$$

Flux expected at E from source at z X-ray LF in X-ray band

f(E): normalized spectrum of the source
with unit luminosity in the X-ray band

- AGN have different spectral shapes depending on e.g. obscuration

$$I(E) = I(E)_{unabs} + I(E)_{abs}$$

Here comes our knowledge from X-ray surveys of the ‘evolutionary’ properties (i.e., vs. z and L) and relative fractions of unabs and abs AGN

$$I_X = \int_0^{\infty} I(E) dE$$

Total X-ray intensity (by integrating over energy)

The Soltan argument and the SMBH accretion history information ‘stored’ in the XRB. II

- The total intensity is derived converting the X-ray intensity into a bolometric one assuming a bolometric correction ($f_{bol,X}$)

$$I_T = f_{bol,X} I_X$$

$$(1 + \langle z \rangle) \frac{4\pi I_T}{c} = (1 + \langle z \rangle) u_X^* = u_X$$

\downarrow \rightarrow

u*: observed energy density u: comoving energy density

- Consider the obscured AGN fraction f_{obs} and report the total intensity in terms of unobscured AGN

$$f_{obs} = N_{abs}/N_{unabs} \rightarrow N_{abs} = f_{obs} N_{unabs}$$

$$I_X = I_{unabs} + I_{abs} = I_{unabs} + f_{obs} I_{unabs} = I_{unabs}(1 + f_{obs})$$

$$I_T = f_{bol,X} (1 + f_{obs}) I_{X,unabs}$$

The Soltan argument and the SMBH accretion history information ‘stored’ in the XRB. III

$$u_X^* = (1.0 - 2.3) \times 10^{-15} \text{ erg cm}^{-3}$$

after Elvis et al. (2002)

$$\rho_{BH,X} = \frac{1-\eta}{\eta c^2} (1 + \langle z \rangle) u_X^* = (3.0 - 6.7) \times 10^5 M_\odot \text{ Mpc}^{-3}$$

assuming $\eta=0.1$
and $\langle z \rangle \sim 1$

Besides efficiency, bolometric correction factors and limited knowledge of AGN duty cycle, the observed density of BHs in the local – remnants of active galaxies – is consistent with XRB intensity